GCA-TR-68-4-N

PLANETARY METEOROLOGY

George Ohring Wen Tang Joseph Mariano

Gloria DeSanto*

FINAL REPORT

Contract No. NASW-1574

May 1968

GCA CORPORATION
GCA TECHNOLOGY DIVISION
Bedford, Massachusetts

Prepared for

NATIONAL AERONAUTICS AND SPACE ADMINISTRATION
Headquarters
Washington, D. C.

*Now at National Center for Atmospheric Research, Boulder, Colorado.

TABLE OF CONTENTS

LIST OF ILLUSTRATIONS

PLANETARY METEOROLOGY

By George Ohring, Wen Tang, Joseph Mariano
and Gloria DeSanto
GCA CORPORATION
GCA TECHNOLOGY DIVISION
Bedford, Massachusetts

SUMMARY

The thermal equilibrium model for computing vertical temperature profiles in the Martian atmosphere [1]* is expanded to include water vapor radiative processes. Calculations with this model show that the observed small amount of water vapor in the Martian atmosphere (~10μ percipitable water) does not significantly affect the computed temperature profile. For example, the Martian surface temperature is increased by only 1°K due to the presence of water vapor. Thermal equilibrium calculations of the mean surface temperature and mean vertical temperature profile on Mars indicate that the temperatures are relatively insensitive to variations in surface pressure and carbon dioxide abundance over the range representative of current uncertainties in these parameters. Thus, even with present uncertainties in surface pressure and carbon dioxide abundance, it is possible to obtain good theoretical estimates of Martian surface and atmospheric temperatures. The mean Martian surface temperature is computed to be 216°K, indicating a greenhouse effect of 8°K, which can be compared to a greenhouse effect of 35°K on Earth.

Two models for calculating diurnal variations on Mars are developed. The first model is for calculation of diurnal variations of temperature and includes radiative and eddy heat transfer in the atmosphere and molecular conduction in the soil. A constant eddy mixing coefficient, K, is assumed for the atmosphere. Calculations with $K = 10^4$ cm^2 sec^{-1} indicate that the diurnal range at a height of ~1.5 km is about 12 percent of the surface diurnal range while at ~3 km it is about 3 percent of the surface diurnal range. The second model is for calculation of the diurnal variation of temperatures and winds. In this model K is variable, being a function of height, wind shear, and Richardson number. Some preliminary results of a partially successful computer run with this model are presented.

*Numbers in [ ] represent reference numbers.

1. INTRODUCTION

This final report summarizes research performed during the past year under Contract NASW-1574, Planetary Meteorology, with Headquarters, National Aeronautics and Space Administration. Several problems relating mainly to the meteorology of Mars were undertaken during the course of the year. These included: (a) the effect of the small amount of atmospheric water vapor on Mars on vertical temperature profiles computed with a thermal equilibrium model, (b) the sensitivity of computed Martian temperatures to present uncertainties in carbon dioxide abundance and surface pressure, (c) the application of radiative transfer theory to the problem of theoretically determining the thermal structure of a planetary atmosphere, and (d) diurnal variations of temperature and wind on Mars. Except for item (c), these studies and the results obtained are described in detail in the remainder of this report. Item (c) in the subject of a technical report [4] that has already been published under the contract; therefore, only an abstract is included in the present final report.

2. THERMAL EQUILIBRIUM CALCULATIONS FOR THE MARTIAN ATMOSPHERE

2.1 Introduction

In Ohring, et al. [1] results were presented on the seasonal and latitudinal variations of the average surface temperature and vertical profile of atmospheric temperature on Mars, as computed with a thermal equilibrium model. The model atmosphere used for the computations had a surface pressure of 10 mb, consisted of 60 percent (by mass) CO_2, and contained no water vapor. In reality, the Martian atmosphere does contain water vapor, although in small amounts. Also, the surface pressure and CO_2 content are somewhat uncertain at the present time. In the present study, the effects of water vapor and the uncertainties in surface pressure and CO_2 content are evaluated with respect to the temperatures computed with a thermal equilibrium model. To accomplish this, techniques must first be developed for including infrared emission and solar absorption by water vapor in the thermal equilibrium model.

2.2 Expansion of Thermal Equilibrium Model to Include Water Vapor

The requirements for thermal equilibrium [1,3] may be summarized as follows:

(1) At the top of the atmosphere — A balance is required between net incoming solar radiation and outgoing long-wave radiation.

(2) Within the atmosphere — For those layers in which radiative energy exchange leads to a radiative equilibrium temperature lapse rate that is less than a prescribed convective lapse rate, local radiative equilibrium is assumed. For those layers in which radiative energy exchange would lead to a temperature lapse rate greater than the prescribed critical convective lapse rate, a balance is assumed between the radiative energy loss and the amount of convective energy required to maintain the critical convective lapse rate.

(3) At the surface — A balance is required between the net radiative energy gain and the convective energy loss. The convective energy loss is equal to the amount of heat that must be transferred to the atmosphere to prevent the formation of a super-convective lapse rate.

Thus, the thermal equilibrium model includes the effect of convective processes — that is, the elimination of unstable layers — without dealing with the actual dynamics of convection. The equations describing these equilibrium conditions may be found in Ohring, et al. [1]. The thermal

equilibrium temperature profile is computed using an iterative procedure based upon the initial value method of computing radiative equilibrium temperatures.

The radiative rates of temperature change, which are required in the model, depend upon two factors: infrared cooling and solar heating. Thus,

$$\left(\frac{\partial\theta}{\partial t}\right)_{rad} = \left(\frac{\partial\theta}{\partial t}\right)_{IR} + \left(\frac{\partial\theta}{\partial t}\right)_{s} \tag{1}$$

where θ is temperature. For computation of the infrared cooling rates, the model of Rodgers and Walshaw [4] is used. The infrared cooling rates at level z due to a spectral interval of an absorption band is given by

$$\left(\frac{\partial\theta}{\partial t}\right)_{IR} = -\frac{g}{c_p p}\left[B(Z)\,\frac{dT}{dz}(z,Z) - \int_o^Z \frac{dT}{dz}(z,z')\,\frac{dB}{dz'}(z')\,dz'\right] \tag{2}$$

where z, the vertical coordinate, is given by $z = \ell n\ \varphi$; $\varphi = p/p_o$, the ratio of atmospheric pressure at level z to surface pressure; g is the gravitational acceleration; c_p is the specific heat at constant pressure; B is the blackbody flux for the spectral interval; Z is the highest level considered; and T is the transmission function for the absorption band.

Water vapor has two major absorption bands in the infrared — the 6.3μ band and the rotation band at wavelengths greater than 16μ. For the low temperatures in the Martian atmosphere, most of the blackbody energy is found at the higher wavelengths. For example, at a temperature of 200°K, only 2 percent of the energy is below $\lambda = 8\mu$, whereas over 65 percent of the energy is above $\lambda = 16\mu$. Thus, for the calculations we may assume that only the water vapor rotational band is of importance on Mars.

The transmittance for a spectral interval within the water vapor rotational band may be written as [4]

$$T(z,z') = \exp\left[-\frac{1.66\ k\bar{m}}{\delta}\left(1 + \frac{1.66\ k\bar{m}}{\pi\,\bar{\alpha}}\right)^{-\frac{1}{2}}\right] \tag{3}$$

where $\bar{\alpha}$ is the mean half-width of an absorption line along the atmospheric path, k is the mean line intensity, $\bar{m}$ is the amount of water vapor in g cm^{-2} along the path, δ is the mean line spacing, and the factor 1.66 is introduced as a multiple of $\bar{m}$ to approximate flux transmission.

Letting $A = 1.66k/\delta$ and $B = 1.66k/\pi$, we have

$$T(z,z') = \exp\left[-A\bar{m}\left(1 + \frac{B\bar{m}}{\bar{\alpha}}\right)^{-\frac{1}{2}}\right] . \tag{4}$$

The mean half-width between two levels is obtained with the use of the Curtis-Godson approximation.

$$\bar{\alpha} = \frac{\alpha_s}{2}\left(\frac{\theta_s}{\theta}\right)^{\frac{1}{2}}\left(\frac{p_o}{p_s}\right)\left[\frac{\varphi(z)^2 - \varphi(z')^2}{\varphi(z) - \varphi(z')}\right] \tag{5}$$

where α_s is the half-width at standard pressure, p_s, and standard temperature, θ_s; and θ is a representative temperature of the Martian atmosphere, assumed to be 200°K. The amount of water vapor between two levels includes a correction, following Rodgers and Walshaw [4], for the effect of temperature on line intensities.

$$\bar{m} = \frac{\Phi(\theta) w p_o}{g}\left[|\varphi(z) - \varphi(z')|\right] \tag{6}$$

where w is the mass mixing ratio of water vapor, and

$$\log_e \Phi(\theta) = a(\theta - 260) + b(\theta - 260)^2 \tag{7}$$

where $\theta = 200°K$, a temperature representative of the Martian atmosphere. The assumption of a constant temperature for the temperature correction to both half-width and absorber amount simplifies the computations. The errors introduced by this assumption are much smaller than the errors introduced by uncertainties in water vapor mixing ratios on Mars.

For evaluation of Equation (2), dT/dz is required.

$$\frac{dT}{dz} = \frac{\partial T}{\partial \bar{m}}\frac{d\bar{m}}{dz} + \frac{\partial T}{\partial \bar{\alpha}}\frac{d\bar{\alpha}}{dz} \tag{8}$$

$$\frac{d\bar{m}}{dz} = \frac{dm}{d\varphi}\frac{d\varphi}{dz} = \pm\varphi\ \Phi(\theta)\frac{w p_o}{g} \quad \begin{matrix}\varphi > \varphi' \\ \varphi < \varphi'\end{matrix} \tag{9}$$

$$\frac{d\bar{\alpha}}{dz} = \frac{d\bar{\alpha}}{d\varphi}\frac{d\varphi}{dz} = -\varphi\frac{\alpha_s}{2}\left(\frac{\theta_s}{\theta}\right)^{\frac{1}{2}}\frac{p_o}{p_s} \tag{10}$$

$$\frac{\partial T}{\partial \bar{m}} = -A\left(1 + \frac{B\bar{m}}{\bar{\alpha}}\right)^{-\frac{3}{2}}\left(1 + \frac{\bar{m}B}{2\bar{\alpha}}\right)\exp\left[-A\bar{m}\left(1 + \frac{B\bar{m}}{\bar{\alpha}}\right)^{-\frac{1}{2}}\right] \tag{11}$$

$$\frac{\partial T}{\partial \bar{\alpha}} = -\frac{AB\bar{m}^2}{2\bar{\alpha}^2}\left(1 + B\frac{\bar{m}}{\bar{\alpha}}\right)^{-\frac{3}{2}}\exp\left[-A\bar{m}\left(1 + \frac{B\bar{m}}{\bar{\alpha}}\right)\right]^{-\frac{1}{2}} \tag{12}$$

The appropriate constants for the spectral intervals of the rotational water vapor band are listed in Table 1.

The expression for the half-width, Equation (5), implicitly assumes that Doppler broadening is negligible compared to Lorentz broadening. The height in the Martian atmosphere at which Doppler broadening starts to become important can be determined from the following equation (see References 2 and 4).

$$y\eta \sqrt{\pi} \exp[- y^2(\eta - 1)] = 1 \tag{13}$$

where $y = \alpha_L/\alpha_D$, the ratio of Lorentz half-width to Doppler half-width; and $\eta = kwp_s/2\pi\alpha_{L_s}g$. For the stronger spectral intervals, for example, No. 3, and for a water vapor amount of 10μ precipitable water, which is equivalent to a mixing ratio of 3.73×10^{-5}, η is about 3×10^3. From Equation (13), this value of η leads to a value of about 0.04 for y. Since α_D is 5×10^{-4} cm^{-1} [4], $\alpha_L = 2 \times 10^{-5}$ cm^{-1}. The pressure level in the Martian atmosphere corresponding to this value of α_L is

$$p = \frac{\alpha_L}{\alpha_{L_s}} p_s = \frac{2 \times 10^{-5}}{5 \times 10^{-2}} \times 10^3 = 4 \times 10^{-1} \text{ mb} . \tag{14}$$

For a Martian atmosphere scale height of 9 km and surface pressure of 10 mb, this corresponds to a height of 29 km.

To evaluate Equation (2), expressions for B, the blackbody flux in a spectral interval, are required. The blackbody flux in any spectral interval may be written as

$$B = \pi \int_{\nu_1}^{\nu_2} \frac{c_1 \nu^3 d\nu}{\exp\left(c_2 \frac{\nu}{\theta}\right) - 1} \tag{15}$$

where ν is wavenumber, B_ν is the Planck intensity, $c_1 = 1.1909$ ergs $cm^{-2} sec^{-1}$ $ster^{-1}$, $c_2 = 1.4389$ cm deg^{-1}, and θ is temperature. With the substitution, $v = c_2\nu/\theta$, Equation (15) becomes

$$B = \frac{\pi c_1 \theta^4}{c_2^4} \int_{v_1}^{v_2} \frac{v^3 dv}{e^v - 1} . \tag{16}$$

TABLE 1

CONSTANTS FOR WATER VAPOR ROTATIONAL BAND [4]

Spectral Region	Spectral Interval	k/δ g^{-1} cm^2	$\pi\alpha_o/\delta$	a 10^{-3} deg^{-1}	b 10^{-6} deg^{-2}
1	0-40	579.75	0.093	-6.75	8.55
2	40-160	7210.3	0.182	-2.93	2.01
3	160-280	6024.8	0.094	1.43	-13.0
4	280-380	1614.1	0.081	9.59	-41.8
5	380-500	139.03	0.080	14.3	-23.7
6	500-600	21.64	0.068	15.2	-30.1

Equation (16) can be broken down to

$$B = \frac{\pi c_1 \theta^4}{c_2^4} \left[\int_0^{v_2} \frac{v^3 dv}{e^v - 1} - \int_0^{v_1} \frac{v^3 dv}{e^v - 1} \right] . \tag{17}$$

For $v \leq 3.5$,

$$\int_0^v \frac{v^3 dv}{e^v - 1} \simeq v^3 \left(\frac{1}{3} - \frac{v}{8} + \frac{v^2}{60} - \frac{v^4}{5040} + \frac{v^6}{272160} - \frac{v^8}{13,305,600} \right) . \tag{18}$$

For $v > 3.5$

$$\int_0^v \frac{v^3 dv}{e^v - 1} \simeq \left[\frac{\pi^4}{15} - \sum_{m=1}^{3} \frac{e^{-mv}}{m^4} \left([(mv + 3)mv + 6]mv + 6 \right) \right] \tag{19}$$

(see Reference 5).

The total infrared cooling due to water vapor is the sum of the cooling rates in each of the spectral intervals computed from Equation (2). The downward flux at the surface in the water vapor band is computed in a manner similar to that used for CO_2 [1] except that the appropriate transmissions and blackbody energy for water vapor are used.

The heating of the atmosphere due to absorption of near infrared solar radiation by water vapor is computed using Houghton's [6] method. The average diurnal heating rate at a pressure level p is given by

$$\left(\frac{\partial \theta}{\partial t} \right)_s = \frac{g}{c_p} \overline{\cos \psi} \; r \sum_{\ell} I_{o_\ell} \frac{dA_\ell}{dp} \tag{20}$$

where $\overline{\cos \psi}$ is the average cosine of the solar zenith angle for the day, r is the fraction of the day the sun is shining, I_{o_ℓ} is the intensity of solar radiation per wavenumber in the ℓ-th absorption band, and A_ℓ is the integrated absorption of the ℓ-th band for the atmospheric column extending from the top of the atmosphere to the pressure level p along a slant path parallel to the solar beam, and the summation extends over the near infrared absorption bands of water vapor. Because of the small amount of water vapor on Mars a weak band form for the integrated absorption applies.

$$A_\ell = a_\ell (\bar{p}m)^{\frac{1}{2}} \tag{21}$$

where $\bar{p} = p/2$ (mb), and m is the water vapor path length in precipitable cm. For a water vapor mixing ratio w, the water vapor path length is

$$m = \frac{10^3 w}{g} \overline{\sec \psi}\, p \tag{22}$$

where p is in mb.

For dA_ℓ/dp, we obtain

$$\frac{dA_\ell}{dp} = a_\ell \left(\frac{1}{2} \frac{10^3 w \overline{\sec \psi}}{g} \right)^{\frac{1}{2}} . \tag{23}$$

The values of a_ℓ and $I_{o\ell}$ at Mars mean distance from the sun for the near infrared bands of water vapor are listed in Table 2 [6].

The solar flux reaching the surface is computed as in Ohring, et al.[1] except that the absorption of solar radiation by water vapor can now be included. Thus,

$$S_g = (1 - A) r \overline{\cos \psi} \left(S_o - \sum_\ell I_{o_\ell} A_{g_\ell} \right) \tag{24}$$

where S_g is the amount of solar radiation reaching the surface, A is the Martian planetary albedo, S_o is the intensity of solar radiation at Mars' distance from the sun, the subscript g refers to the surface, and the summation is over the near-infrared bands of both carbon dioxide and water vapor.

These procedures for water vapor radiation effects were incorporated into the thermal equilibrium computer program described in Ohring, et al.[1].

2.3 Effect of Water Vapor on Thermal Equilibrium Calculations

Water vapor was first detected spectroscopically on Mars by Kaplan, Münch, and Spinrad [7]. They detected weak absorption features near 8200Å and derived an abundance of 14±7μ of precipitable water. More recent spectroscopic observations [8] yield typical amounts of water vapor of the order of 10-20μ precipitable water. Photometric observations have yielded 200μ precipitable water [9] and, more recently, 45μ precipitable water [10]. Thus the indications are that the average amount of water vapor on Mars is between 10μ and 100μ with the most probable value closer to 10μ.

TABLE 2

PARAMETERS FOR NEAR-INFRARED ABSORPTION BANDS OF WATER VAPOR [6]

Region (μ)	a	I_o erg cm^{-2} $sec^{-1}(cm^{-1})^{-1}$
6.3	150	3.03
2.7	81	12.6
1.9	40	20.4
1.4	20	28.1
1.1	2	31.0
0.9	2	31.2

The amount of water vapor in precipitable cm of water is given by

$$P.W. = \frac{\int_0^\infty \rho_{H_2O}\, dz}{\rho_w} \tag{25}$$

where ρ_{H_2O} is the water vapor density, and ρ_w is the density of liquid water, $1\ g\ cm^{-3}$. If the water vapor mixing ratio is constant with altitude, Equation (25) can be written as

$$P.W. = \frac{w\int_0^\infty \rho\, dz}{\rho_w} \tag{26}$$

where ρ is the Martian atmospheric density, and w is the water vapor mixing ratio, ρ_{H_2O}/ρ. With the use of the hydrostatic equation, we can obtain the following expression for w.

$$w = \frac{(P.W.)g\ \rho_w}{p_o} \tag{27}$$

where p_o is the surface pressure. A value of 10μ of precipitable water corresponds to a mixing ratio of 3.73×10^{-5}; 100μ corresponds to $w = 3.73 \times 10^{-4}$.

To evaluate the effect of water vapor, calculations of the mean daily vertical temperature profile were performed for 80°S latitude at the time of the southern hemisphere summer solstice (δ, solar declination, = -24°) and for a surface pressure of 10 mb. A four-layer atmosphere computing model is used. An albedo of 30 percent is assumed and a value of 0.269 for $(\gamma-1)/\gamma$, where γ is the ratio of the specific heat at constant pressure to the specific heat at constant volume, is used. Five different experiments were performed for various combinations of carbon dioxide and water vapor abundance. The computed surface temperatures for these five experiments are listed in Table 3. The first experiment indicates that a surface temperature of 254.0°K is obtained without including water vapor. The second experiment indicates the effect of 10μ of precipitable water — an amount consistent with the available observations. This amount of water vapor increases the Martian greenhouse effect only slightly, the new surface temperature being 254.5°K. In the third experiment, the assumed water vapor amount is 100μ precipitable water, or 10 times the observed amount. The computed surface temperature is 255.5°K, only 1.5°K higher than in the pure

TABLE 3

COMPUTED MARTIAN SURFACE TEMPERATURES FOR VARIOUS COMBINATIONS OF CO_2 AND H_2O AMOUNTS

(LATITUDE -80°; SOLAR DECLINATION -24°)

Experiment No.	Mixing Ratios		Computed Surface Temperature (°K)
	CO_2	H_2O	
1	0.6	0	254.0
2	0.6	0.373×10^{-4}	254.5
3	0.6	0.373×10^{-3}	255.5
4	0	0.373×10^{-4}	244.9
5	0	0.373×10^{-3}	245.7

CO_2 case. These results indicate that water vapor plays only a minor role in the Martian greenhouse effect, carbon dioxide playing the major role. Experiments 4 and 5 show the surface temperature that would be obtained if only water vapor contributed to the Martian greenhouse effect. The surface temperature would drop some 10°K to about 245°K. This temperature is within a degree of the radiative equilibrium temperature that Mars would have at this location and time in the absence of any infrared absorbing molecules in its atmosphere.

The vertical temperature profiles with and without water vapor also show only small differences. In Figure 1 is shown a comparison between two temperature profiles — one for carbon dioxide alone, the other for carbon dioxide plus 100μ of precipitable water. Although the temperatures in the lower atmosphere are slightly increased by the presence of water vapor, temperatures in the upper atmosphere are slightly decreased.

Figure 2 shows a comparison between a temperature profile computed with both carbon dioxide and water vapor, and one for water vapor alone. With water vapor alone, the temperatures are about 10 degrees lower at all levels.

These results indicate that water vapor plays only a minor role in determining the surface temperature and vertical temperature profile on Mars. Thus, the Martian seasonal and latitudinal temperature variations computed by Ohring, et al. [1] would not be significantly changed by the inclusion of water vapor radiative effects.

The Martian greenhouse effect is increased by only 1°K due to the presence of water vapor. This is in contrast to the Earth's atmosphere where water vapor plays the dominant role in producing a greenhouse effect of about 35°K.

2.4 Sensitivity of Computed Martian Temperatures to Present Uncertainties in CO_2 Abundance and Surface Pressure

Despite the new information provided by the Mariner IV radio occultation experiment [11] and recent spectroscopic observations [12,13,14], the surface pressure and carbon dioxide abundance on Mars are still somewhat uncertain. A recent analysis of available observations [15] suggests that the surface pressure is in the range 5 to 14 mb and the CO_2 abundance is in the range 55 to 70 m-atm. A question arises as to the sensitivity of computed Martian temperatures to these uncertainties in input parameters. In the present study, we attempt to answer this question,

We have computed vertical temperature profiles using the thermal equilibrium model and computational techniques described in Ohring, et al.[1], as modified for the inclusion of water vapor in Section 2.2 of this report, for three model atmospheres representing a nominal mean surface pressure model,

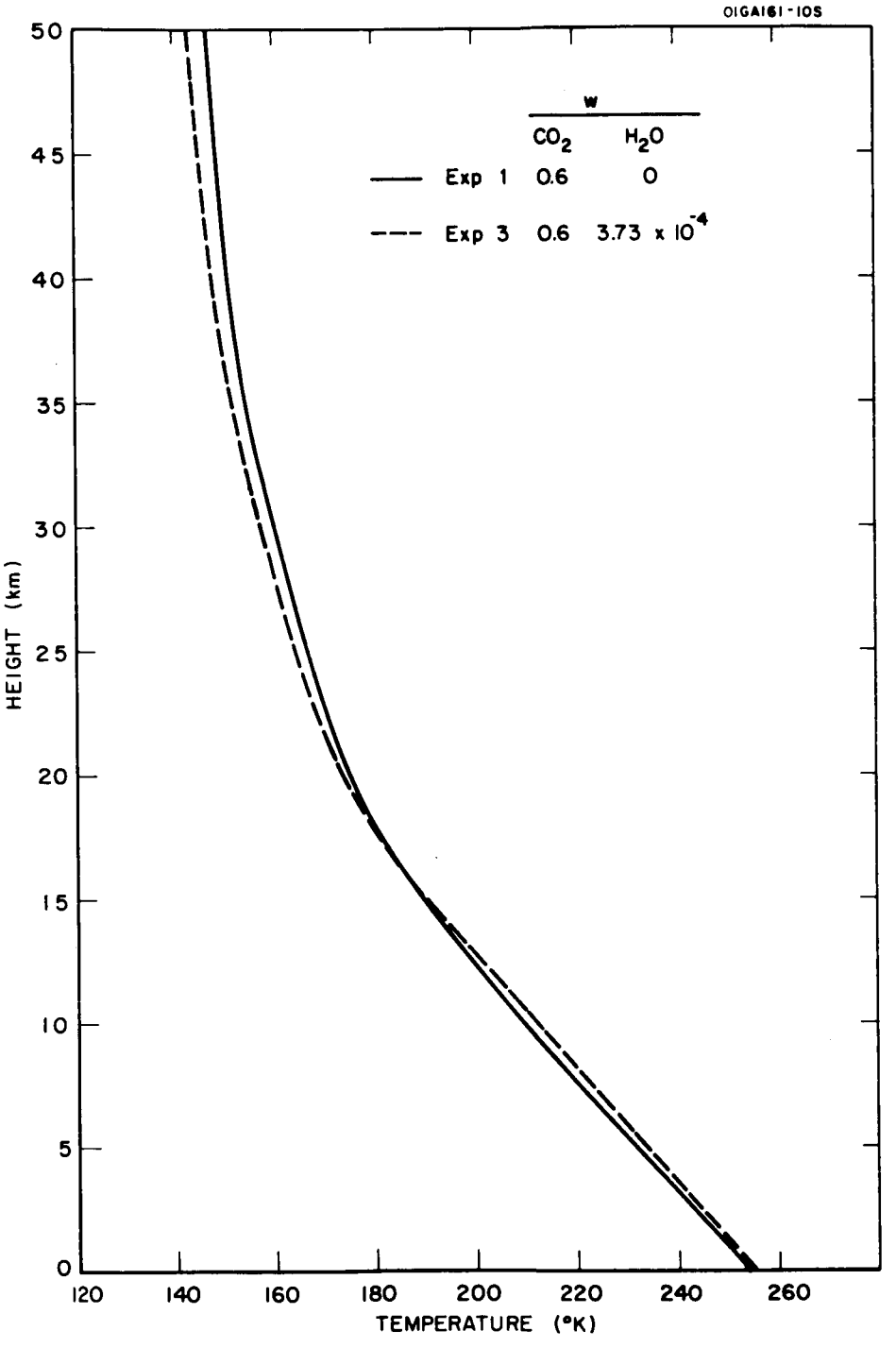

Figure 1. Computed Martian temperature profiles with and without water vapor. (Latitude, -80°; solar declination, -24°)

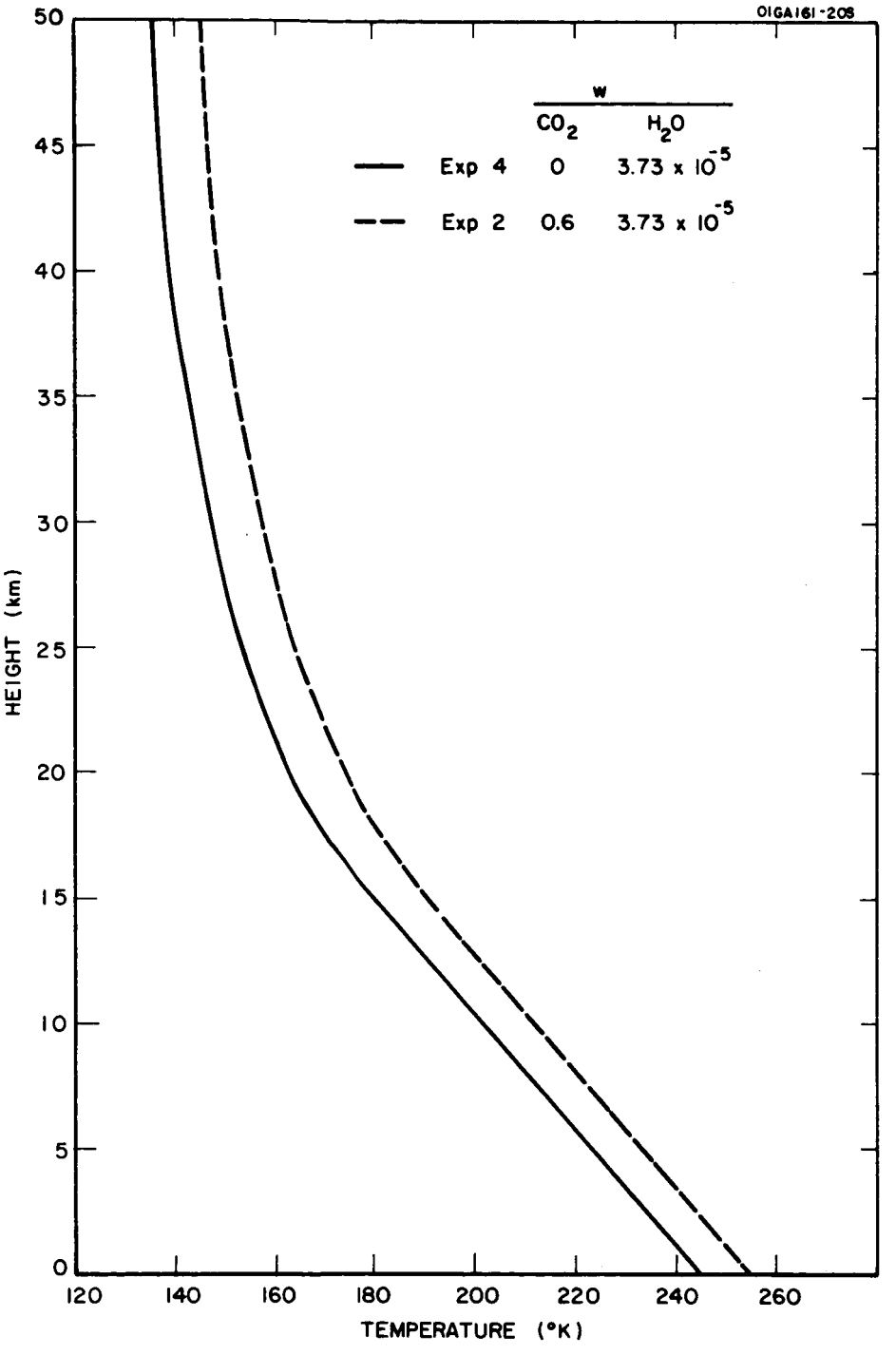

Figure 2. Computed Martian temperature profile with and without carbon dioxide (latitude, -80°; solar declination, -24°).

an upper limit surface pressure model, and a lower limit surface pressure model. Both CO_2 and H_2O radiative effects are included and a four-layer atmospheric model is used for the computations. All calculations are performed for the mean annual condition of solar insolation on Mars and for an albedo of 0.30. The computed temperature profile is thus a theoretical estimate of the mean annual vertical temperature profile, or standard atmosphere temperature profile, for Mars.

As the composition of a planetary atmosphere changes, so do such thermodynamic constants as the ratio of specific heats, the adiabatic lapse rate, and the molecular weight of the atmosphere. To separate the effect of these changes on the temperature profile from the effect of changes solely due to pressure and CO_2 abundance, two sets of calculations were performed. In the first set, the surface pressure and CO_2 abundance were varied but the thermodynamic constants were assumed equal to those of the nominal mean surface pressure model. In the second set, thermodynamic constants appropriate to each of the pressure-composition models were used. In both sets of experiments, it is assumed that nitrogen is the other component of the atmosphere.

The physical models for the first set of experiments are depicted in Table 4. In this table, p_g is the surface pressure, m is the molecular weight of the atmosphere, γ is the ratio of the specific heat at constant pressure of the specific heat volume, c_p is the specific heat at constant pressure, and Γ_{ad} is the adiabatic lapse rate.

The computed temperature profiles for this set are shown in Figure 3. They are quite similar, indicating that variations of CO_2 abundance and surface pressure over the range currently associated with the uncertainties in these parameters changes the greenhouse effect and thermal equilibrium temperatures only slightly. The lowest surface temperature (215.4°K) occurs with the 5-mb model, the highest (216.2°K) with the 12-mb model. At upper levels, the temperature for the 5-mb model are a few degrees higher than for the other models. Since the magnitude of the greenhouse effect depends upon the product of CO_2 abundance and surface pressure, and since the 5-mb model has the lowest value of this product, it is to be expected that the surface temperature for this model would be less than for the other models. To maintain a balance between incoming solar radiation and outgoing thermal radiation at the top of the atmosphere, the upper level temperatures for the 5-mb model must then be slightly higher than for the other models. The major point, however, is the relative insensitivity of the temperatures to the variations in CO_2 abundance and surface pressure. The computed surface temperature of 215°K, which represents the mean surface temperature of Mars, is in good agreement with the mean surface temperature deduced from microwave observations: 220°K±15°K[15].

In the second set of computations, thermodynamic constants appropriate to each of the pressure-composition models were used. The physical models for the second set of computations are depicted in Table 5. The computed thermal equilibrium temperature profiles are shown in Figure 4. Changes

TABLE 4

PHYSICAL MODELS FOR FIRST SET OF EXPERIMENTS

Exp. No.	p_g (mb)	CO_2 % by Mass	CO_2 Abundance (m-atm)	m	$\frac{\gamma-1}{\gamma}$	c_p (erg $g^{-1}deg^{-1}$)	Γ_{ad} (°K/km)	H_2O Mixing Ratio
1	9	0.61	74	35.8	0.268	8.54×10^6	4.4	3.73×10^{-5}
2	5	1.00	68	"	"	"	"	"
3	12	0.28	46	"	"	"	"	"

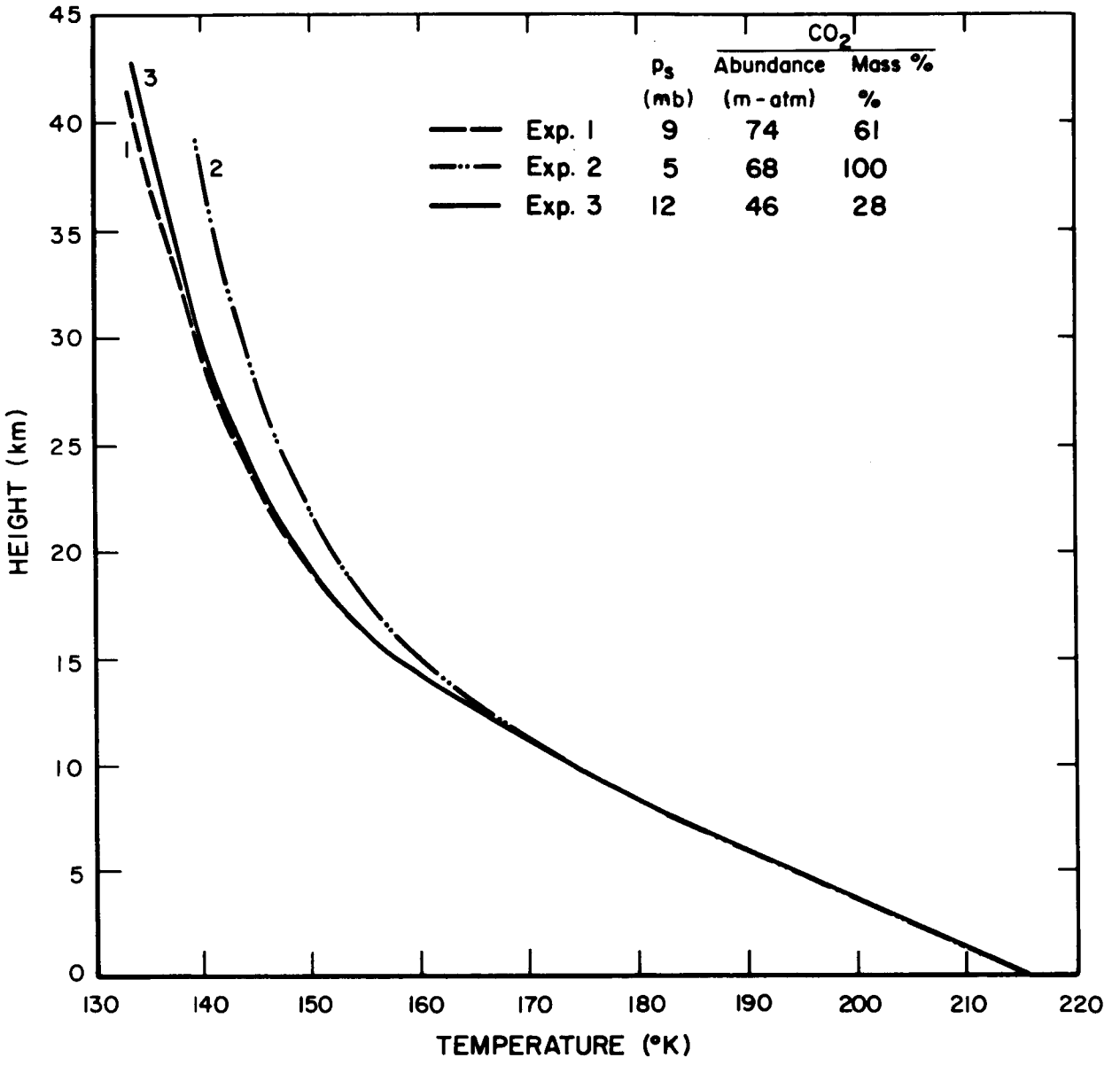

Figure 3. Computed mean vertical temperature profiles on Mars for three carbon dioxide and surface pressure combinations. Thermodynamic constants used in computations are those of Experiment 2.

TABLE 5

PHYSICAL MODELS FOR SECOND SET OF EXPERIMENTS

Exp. No.	p_g (mb)	CO_2 % by Mass	CO_2 Abundance (m-atm)	m	$\frac{\gamma-1}{\gamma}$	c_p (erg $g^{-1}deg^{-1}$)	Γ_{ad} (°K/km)	H_2O Mixing Ratio
4	9	0.61	74	35.8	0.268	8.54×10^6	4.4	3.73×10^{-5}
5	5	1.00	68	44	0.257	7.36×10^6	5.1	"
6	12	0.28	46	31.2	0.278	9.54×10^6	3.9	"

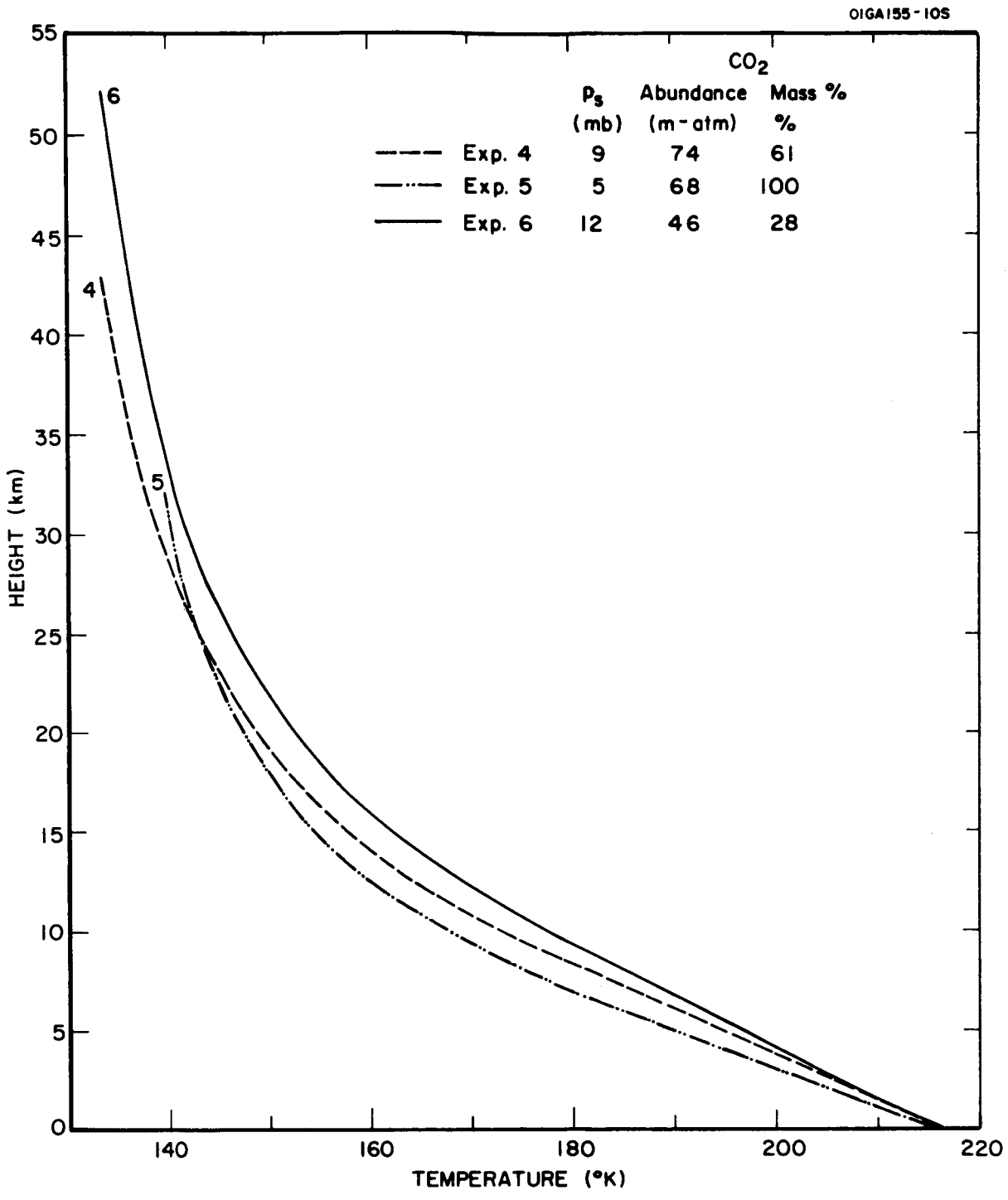

Figure 4. Computed mean vertical temperature profiles on Mars for three carbon dioxide and surface pressure combinations. Thermodynamic constants used in the computations are those appropriate for each experiment.

in the thermodynamic constants and molecular weight affect the adiabatic lapse rate and the scale height of the atmosphere. Thus, the differences in these three temperature versus height profiles are a result of both a change in the magnitude of the greenhouse effect and changes in the adiabatic lapse rate and atmospheric scale height. The surface temperatures remain the same as those computed for the first set. The vertical profiles differ somewhat more than they do for the first set due to the inclusion of the appropriate adiabatic lapse rate and molecular weight for each model atmosphere. But again, the major finding is the relative insensitivity of the thermal equilibrium temperature profiles to variations in model atmosphers for Mars that cover the range of present uncertainties in surface pressure and CO_2 abundance.

These results indicate that even with current uncertainties in CO_2 abundance and surface pressure, it is possible to obtain good estimates of average Martian surface and atmospheric temperatures. Such estimates are needed for design of space probes to Mars. If it were the other way around — that is, if the vertical temperature structure was extremely sensitive to variations in surface pressure and carbon dioxide abundance — the engineering applications of theoretical estimates of temperature would be limited.

It is of interest to compare the magnitude of the Martian greenhouse effect, as computed from this thermal equilibrium model for mean annual conditions, with the magnitude of the greenhouse effect on Earth. The magnitude of the greenhouse effect may be defined as the increase in surface temperature above its radiative equilibrium value in the absence of an infrared absorbing atmosphere. On Earth, the average surface temperature in the absence of an atmosphere would be 252°K. Largely due to presence of water vapor, in an amount over 10^3 greater than the Martian water vapor abundance, a greenhouse effect of about 36°K is produced. Thus, the observed average surface temperature on Earth is 288°K. On Mars, the average surface temperature in the absence of an atmosphere would be about 208°K. The presence of carbon dioxide, in an amount about 30 times its abundance on Earth, causes a greenhouse effect of about 8°K.

Another interesting comparison may be made between a temperature profile computed on the basis of thermal equilibrium and one computed on the basis of pure radiative equilibrium. Figure 5 shows such a comparison. Both profiles were computed using the physical parameters of experiment 1 and are, therefore, representative of average conditions on Mars. The surface temperature of the pure radiative equilibrium profile is only a few tenths of degree higher than the thermal equilibrium surface temperature. At all levels in the atmosphere, however, the pure radiative equilibrium temperatures are lower than the thermal equilibrium temperatures. A super-adiabatic lapse rate is present in the lower layers of the radiative equilibrium profile. These differences are due to convection, which is taken into consideration in the thermal equilibrium calculations but not in the radiative equilibrium calculations.

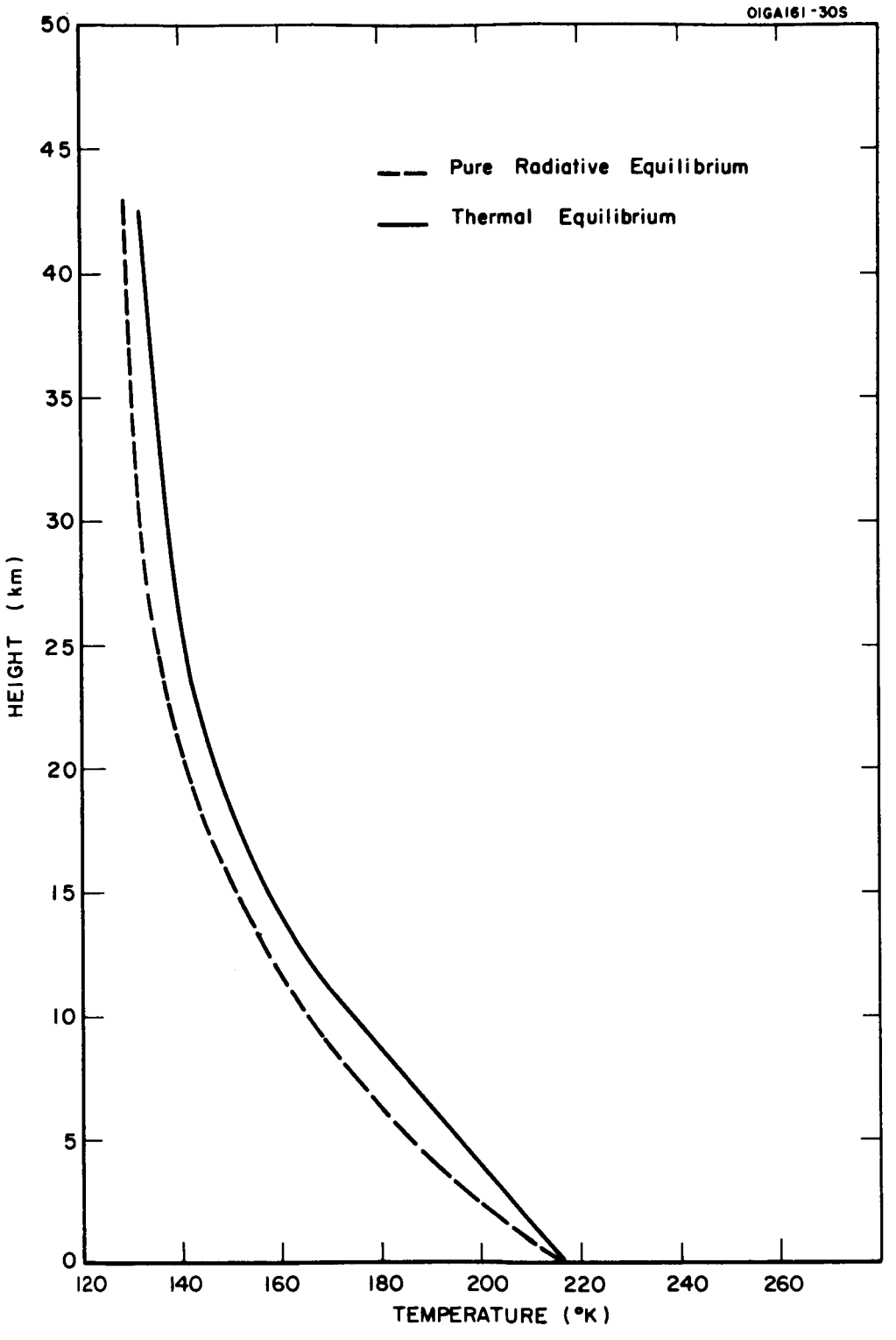

Figure 5. Comparison of thermal equilibrium and radiative equilibrium temperature profiles for Mars.

In Table 6 are listed the magnitudes of the various terms that determine the surface temperature of the thermal equilibrium model for the mean annual condition on Mars. It is quite obvious that the surface temperature is controlled by the solar flux reaching the surface. The convective flux is almost two orders of magnitude less, and the total downward infrared flux, $F\downarrow_{tot}$, almost one order of magnitude less, then the solar flux. On Earth, the convective lux is about 1/5 of, and the downward infrared flux about twice, the solar flux absorbed at the surface [16], a consequence of the much greater greenhouse effect on Earth. On Mars, the downward infrared flux due to water vapor is one order of magnitude less than that due to carbon dioxide. On Earth, the situation is reversed and the downward flux due to water vapor is greater than that due to carbon dioxide.

2.5 Conclusions

The small smount of water vapor on Mars plays only a minor role in the radiative transfer of heat in the Martian atmosphere. As a result, the surface temperature and vertical temperature profile are not significantly changed by including water vapor in calculations with a thermal equilibrium model. For example, the Martian surface temperature is increased by only 1°K due to the presence of water vapor. This is in contrast to the Earth's atmosphere where water vapor plays the dominant role in producing a greenhouse effect of about 35°K.

Thermal equilibrium calculations of the mean surface temperature and mean vertical temperature profile on Mars indicate that the temperatures are relatively insensitive to variations in surface pressure and carbon dioxide abundance over the range representative of current uncertainties in these parameters. Thus, even with present uncertainties in surface pressure and carbon dioxide abundance, it is possible to obtain good estimates of average Martian surface and atmospheric temperatures.

Compared to a greenhouse effect on Earth of about 35°K, the average Martian greenhouse effect is computed to be 8°K. The downward infrared energy flux at the Martian surface is almost one order of magnitude less than the solar energy flux absorbed at the surface. On Earth, the downward infrared flux is about twice the solar energy flux absorbed at the surface.

TABLE 6

MAGNITUDES OF TERMS IN SURFACE
HEAT BALANCE EQUATION
(ergs cm^{-2} sec^{-1})

Solar Flux	σT^4	Convective Flux	$F\downarrow_{CO_2}$	$F\downarrow_{H_2O}$	$F\downarrow_{tot}$
1.0×10^5	1.2×10^5	1.6×10^3	2.1×10^4	1.6×10^3	2.2×10^4

3. RADIATIVE TRANSFER AND THE THERMAL STRUCTURE OF PLANETARY ATMOSPHERES

The principal investigator was invited to present a review paper on the above subject at the Survey Symposium on Radiation at the XIV General Assembly of the International Union of Geodesy and Geophysics, September 25-October 7, 1967, Switzerland. Most of the literature research required to prepare this paper was performed under the current contract. The paper reviews recent applications of radiative transfer theory to the problem of theoretically estimating the mean surface temperature and mean vertical temperature profile of the planets Earth, Mars, and Venus. It has been published as a Technical Report, GCA-TR-67-18-N, under the current contract and, therefore, is not included in this final report. An abstract of this paper follows.

RADIATIVE TRANSFER AND THE THERMAL STRUCTURE OF PLANETARY ATMOSPHERES

By George Ohring

ABSTRACT

The mean surface temperature and mean vertical distribution of temperature of a planetary atmosphere are, to a large extent, determined by radiative processes. Given the basic physical characteristics of the planetary atmosphere, such as composition, surface pressure, and albedo, it is possible through the application of radiative transfer theory, to compute the temperature structure of the planetary atmosphere. For the Earth's atmosphere the problem has been to determine theoretically the mean vertical temperature profile from the surface up to the thermosphere. An additional problem, related to climatic change, is the effect of changes in the basic physical characteristics, such as composition or cloudiness, on surface and atmospheric temperatures. Application of radiative transfer theory to the atmospheres of the other planets have been aimed at deriving estimates of surface and atmospheric temperatures on Mars and estimates of the greenhouse effect on Venus. The theoretical models and results of recent studies of these topics are reviewed in the present survey paper.

4. DIURNAL VARIATIONS ON MARS

4.1 Introduction

Earth-based infrared window observations of the thermal emission from Mars indicate that the diurnal temperature variation of the Martian surface is about 100°K [17]. This is five to ten times the diurnal temperature range of the Earth's surface. The question arises of how much of this diurnal range is imparted to the Martian atmosphere, and to what heights it propagates. For if a large part of the surface temperature range is propagated to heights of the order of kilometers, Martian meteorology would be significantly affected. Associated with such large diurnal temperature changes would be pressure variations and wind variations. In such a case, the diurnal period would have the same significance as does the annual cycle. This would represent a major difference from Earth, where the diurnal period is only of consequence to small scale meteorological variations, which are of concern to micrometeorologists who study the near surface atmosphere but not to meteorologists concerned with the large-scale dynamics of the atmosphere. Since there are no observations of the diurnal range of temperature in the Martian atmosphere, one must attack the problem theoretically.

On Earth the diurnal temperature wave is propagated upwards largely by an eddy conduction process, radiative processes being relatively unimportant. In such a conduction process, the amplitude of the diurnal wave decreases exponentially with altitude. At a height of one kilometer on Earth, the diurnal temperature range is negligible. On Mars, there are theoretical indications that the diurnal temperature wave propagates to higher altitudes. In a study of radiative relaxation times, Goody and Belton [18] find that radiative processes in the Martian atmosphere are extremely rapid compared to the Earth's atmosphere. As a result, they suggest that radiative processes will cause a propagation of the diurnal temperature wave to greater altitudes on Mars. They suggest a dual wave pattern. One wave near the surface where eddy diffusion dominates; the other wave away from the surface where radiation dominates. They indicate that the entire Martian troposphere has an average diurnal variation of 20 percent of that at the surface.

The only other work on diurnal variations in the Martian atmosphere has been performed by Neubauer [19] and Leovy [20]. Neubauer assumes that radiative transfer can be neglected and that the diurnal wave on Mars is propagated upward by an eddy diffusion process. In the light of Goody and Belton's [18] results, this would appear to be a dangerous assumption. He further assumes that the eddy diffusion coefficient, K, is only a function of height and does not vary with time. For the K(z) dependence, he adapts one used by Fisher [21] for the Earth's atmosphere. With this model, he finds that the diurnal temperature range decreases to 1/5 of its surface value at a height of 0.5 meters. Leovy includes both eddy diffusion and

radiative transport in his calculations. The calculations, however, are for a two-layer atmosphere and the eddy transport from the surface to the lower layer can be represented by a convective term of the form

$$C = h\Delta T$$

where h is a constant, and ΔT is the temperature difference between the surface and the base of the lower layer, 5 m. The value of h was estimated from the observed diurnal variation of temperature at the Martian surface. Eddy exchange between the lower layer and upper layer is assumed to follow a convective term of the form

$$C = h(\Delta T - \Delta T_a)$$

where ΔT is the temperature difference between the two layers, and ΔT_a is the adiabatic temperature difference between the two layers. If ΔT is less than ΔT_a, h is assumed zero; if ΔT is greater than ΔT_a, h is chosen to give a characteristic adjustment time of 10 minutes. With this model, Leovy finds that the diurnal variation decreases to about 1/2 of its surface value at 5 meters and to about 1/3 of its surface value at 3 km. These results are obviously quite different from Neubauer's,and the reasons for the difference quite clearly must lie in one or both of the following factors: (1) Neubauer's neglect of radiative processes; and (2) the differences in treatment of the eddy transport process.

In the present study, we shall develop two models for the calculation of diurnal variations on Mars. Both include radiative and eddy transport processes. The first model assumes that the eddy diffusion coefficient is a constant; only the diurnal variations of temperature are computed with this model. The second model assumes that the eddy diffusion coefficient is a function of height, wind shear, and Richardson's number, and thus, is variable in height and time. This model also includes a computation of the diurnal variation of the wind. In the next section, we discuss the first model.

4.2 Diurnal Variation of Temperature (Constant K Model)

This section describes a model for computing the diurnal variation of temperature in the atmosphere, on the surface, and in the subsurface layer on Mars. It is assumed that atmospheric temperature changes are due to radiative processes and eddy heat transfer processes in the vertical direction. The radiative processes include emission of infrared radiation by the 15μ band of CO_2 and the rotational band of H_2O, and absorption of solar radiation by the near-infrared bands of CO_2 and H_2O. For the eddy heat transfer process, it is

assumed that, K, the coefficient of eddy heat transfer, is constant with altitude and time. This latter assumption is not strictly correct but serves as an approximation to the eddy diffusion process and permits the effect of eddy transport of heat to be compared to the radiative transports. At the surface of the planet, a balance of net radiation, eddy heat exchange with the atmosphere and conductive heat exchange with the subsurface layer is assumed. Temperature changes in the subsurface layer are due to conduction of heat, the thermal diffusivity of the Martian soil being assumed constant with depth and time.

The equation for the rate of temperature change in the atmosphere is

$$\frac{\partial T}{\partial t} = \left(\frac{\partial T}{\partial t} \right)_{IR} + \left(\frac{\partial T}{\partial t} \right)_{S} + \left(\frac{\partial T}{\partial t} \right)_{E} \tag{28}$$

where IR refers to infrared, S to solar, and E to eddy rates of temperature change. Infrared cooling is computed by the method of Rodgers and Walshaw [3] and solar heating by the method of Houghton [6], as described in Ohring, et al.[1] and in Section 2 of this report. The rate of temperature change due to eddy heat transfer can be written as

$$\left(\frac{\partial T}{\partial t} \right)_{E} = \frac{\partial}{\partial z} \left[K \left(\frac{\partial T}{\partial z} + \Gamma \right) \right] \tag{29}$$

where z is height, K is the eddy exchange coefficient and Γ is the adiabatic lapse rate. For constant K, we obtain

$$\left(\frac{\partial T}{\partial t} \right)_{E} = K \frac{\partial^2 T}{\partial z^2} \quad . \tag{30}$$

In the soil only molecular heat conduction is operative and we have for the rate of temperature change at any subsurface level

$$\frac{\partial T'}{\partial t} = k' \frac{\partial^2 T}{\partial z'^2} \tag{31}$$

where the primes refer to soil parameters, k' is the thermal diffusivity of the Martian soil, and z' is depth in the soil.

At the Martian surface, the following balance equation holds:

$$S_g + F\downarrow_g + H_g + G_g = \sigma T_g^4 \tag{32}$$

where the subscript g refers to the surface, S is the solar flux, $F\downarrow_g$ is the downward infrared radiation from the atmosphere, σT_g^4 is the infrared emission by the surface, H_g is the eddy flux of heat between surface and atmosphere, and G_g is the flux of heat between surface and subsurface. The eddy flux of heat can be written as

$$H_g = \rho c_p K \left(\frac{\partial T}{\partial z} + \Gamma \right)_g \tag{33}$$

where ρ is the atmospheric density and c_p is the atmospheric specific heat at constant pressure. The soil flux can be written as

$$G_g = \rho' c' k' \left(\frac{\partial T'}{\partial z'} \right)_g \tag{34}$$

where ρ is the density of the soil and c is the specific heat of the soil. The solar flux and downward infrared radiation at the surface are computed as described in Ohring, et al.[1] except that rather than using the average value of the cosine of the zenith angle for the day, the zenith angle appropriate to the particular time step is used in the computations.

To perform the computations various input parameters are required. As a model Martian atmosphere, we assume one with the following characteristics: surface pressure, 9 mb; CO_2 percentage by mass, 61 percent; H_2O abundance, 10μ precipitable water; mean molecular weight, 35.8; and albedo of 0.30. For the Martian soil parameters, values of $\rho'c' = 1.26 \times 10^7$ erg cm^{-2} deg^{-1} and $k' = 7 \times 10^{-5}$ cm^2 sec^{-1} are assumed. These soil parameters are the same as those derived by Leovy [22] from an analysis of Sinton and Strong's [17] observations of the diurnal variation of Martian surface temperature. An eddy mixing coefficient of $K = 10^4$ cm^2 sec^{-1} is assumed. This value is typical of neutral conditions in the atmospheric boundary layer on Earth. Temperatures are computed at 10 levels in the atmosphere, with 0.9-mb spacing, and at four levels within the soil, with 2-cm spacing. The lowest level within the soil, depth 8.0 cm, is assumed to have a constant temperature, 210°K.

With this model, calculations were performed of the diurnal variation of temperature at the equator for a solar declination of 0° (northern hemisphere spring equinox). Figure 6 shows the computed diurnal variation of temperature at the surface and the first two atmospheric levels. The time coordinate is in Martian hours, with 1 Martian hour defined as 1/24 of a Martian day.

The computed surface temperature variation may be compared to the observed surface temperature variation at the Martian equatorial region measured by Sinton and Strong [17]. The agreement between the computed surface temperatures and those observed by Sinton and Strong, which have errors of perhaps five to ten degrees associated with them, is good.

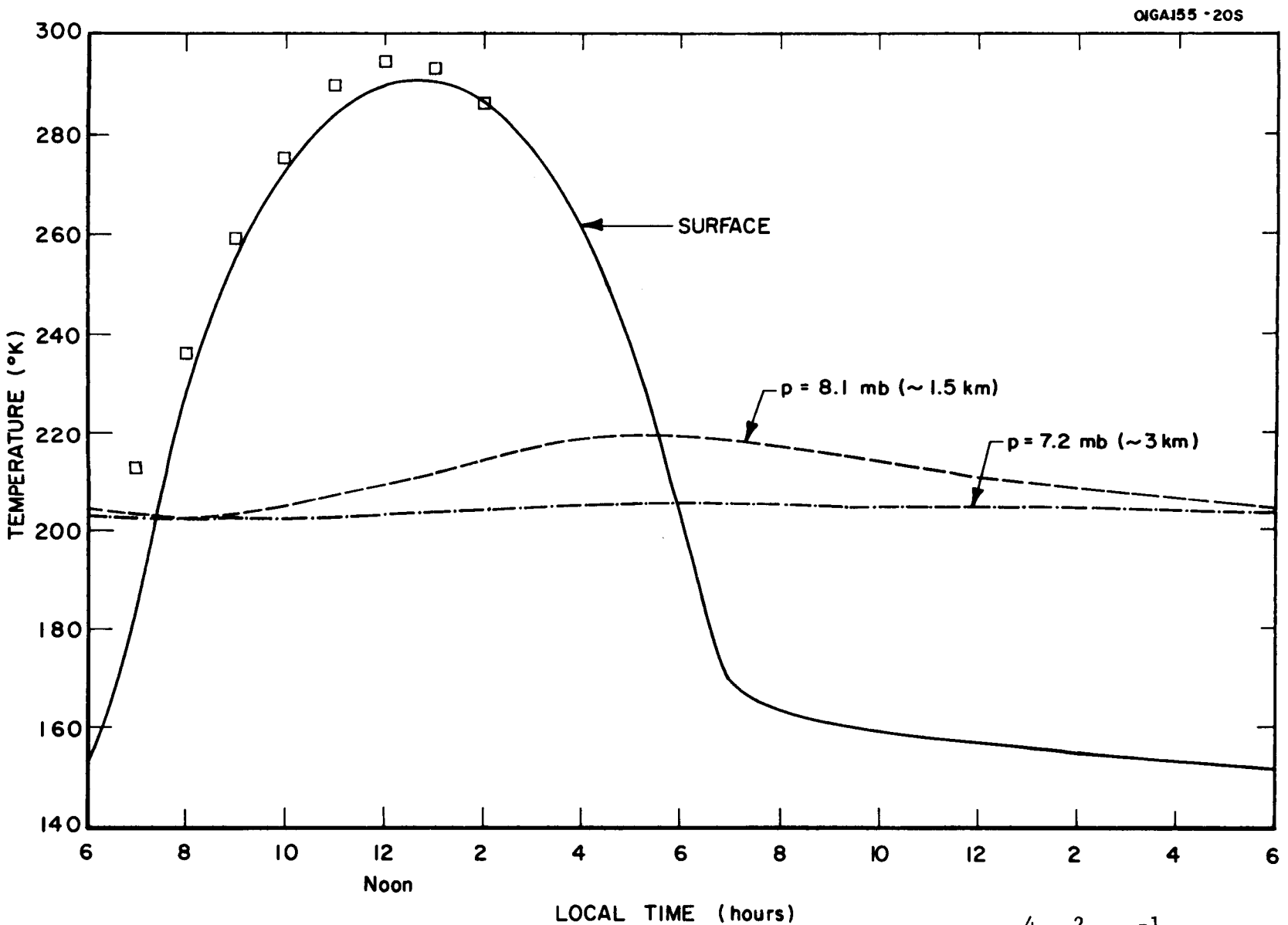

Figure 6. Computed diurnal variation of temperature at equator on Mars ($K = 10^4$ cm^2 sec^{-1}). Plotted points are averages of Sinton and Strong's [17] radiometric observations of surface temperature.

The diurnal range of temperature at 8.1 mb (~1.5 km) is about 12 percent of the range at the surface; at 7.2 mb (~3 km) the diurnal range is about 3 percent of the surface diurnal range. These values can be compared to those that would occur if radiative processes had been neglected in the atmosphere. In such a case, and with constant K, the diurnal wave would propagate by a Fickian diffusion process. The ratio of the diurnal range at height z to that at the surface can then be written as (see, for example, Reference 23)

$$\frac{r(z)}{r(o)} = e^{-\lambda z} \tag{35}$$

where

$$\lambda = \sqrt{\frac{2\pi}{\text{day} \times 2 \times K}} \quad . \tag{36}$$

For $K = 10^4$ cm^2 sec^{-1}, we obtain a ratio of about 1×10^{-4} at a height of 1.5 km, and about 1×10^{-8} at a height of 3 km. This comparison indicates that radiative transfer rather than eddy heat transfer is primarily responsible for propagating the diurnal temperature wave to heights of one to three kilometers on Mars.

The relative importance of radiation and eddy heat transfer can also be ascertained from a comparison of the computed rates of temperature change due to these two processes. Table 7 shows such a comparison for mid-afternoon (3 p.m. local time). It is obvious that the radiative rates of temperature change are at least one order of magnitude greater than the rates of temperature change due to eddy heat transfer at all levels.

The diurnal temperature variation as computed with this model leads to super-adiabatic lapse rates in the lowest three kilometers of the atmosphere during the daytime hours. This is shown in Figure 7, where the vertical profiles of atmospheric temperature are plotted for different times during the day. Also plotted is the slope of the adiabatic lapse rate. In a model in which K is variable, the presence of a super-adiabatic lapse rate would lead to an increase in K. This would cause the diurnal temperature variation to propagate to still greater heights. Thus, there is a feedback mechanism between radiative effects and eddy heat transport. This can only be simulated in a model in which K is permitted to vary. Such a model is discussed in the next section.

4.3 Diurnal Variations of Temperatures and Winds (Variable K Model)

4.3.1 Introduction. — In this section we develop a numerical model for computing the diurnal variations of both temperature and wind on Mars. As discussed in the previous section, the large diurnal variation of surface temperature is propagated through the atmosphere by the combined effects of

TABLE 7

RATES OF TEMPERATURE CHANGE DUE TO RADIATIVE AND EDDY HEAT TRANSFER PROCESSES

Pressure Level (mb)	Height (km)	$\left(\frac{\partial T}{\partial t}\right)_{Rad.}$ (°K/day)	$\left(\frac{\partial T}{\partial t}\right)_{Eddy}$ (°K/day)
8.1	1.4	49	2.0
7.2	2.9	9.3	0.15
6.3	4.5	3.3	0.014
5.4	6.4	1.7	-0.0028
4.5	8.9	0.4	0.020
3.7	10.8	1.4	0.011
2.8	13.7	1.5	0.021
1.9	17.5	1.7	0.015
1.0	23.3	2.6	0.0083

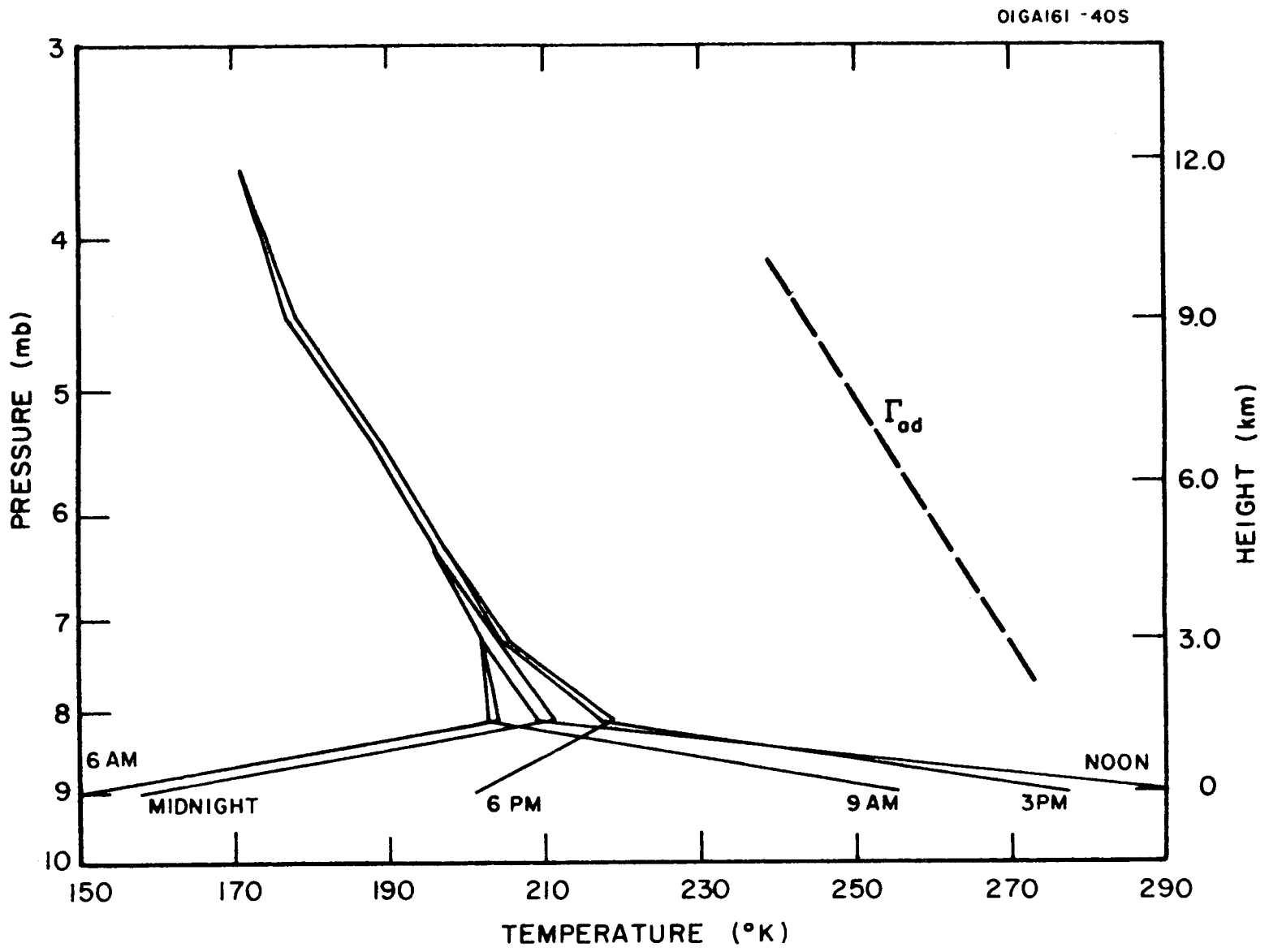

Figure 7. Computed vertical profiles of temperature at Martian equator for different times during the Martian day ($K = 10^4$ cm^2 sec^{-1}).

radiative transfer and eddy heat transfer. As a result of the diurnal variation of atmospheric temperatures, there will be a diurnal variation of the eddy momentum transport coefficient, K, since this coefficient depends upon the thermal structure of the atmosphere. With a diurnal variation of K there will be a diurnal variation of the winds. If the diurnal temperature wave extends to high enough altitudes (of the order of kilometers), a significant diurnal variation in horizontal pressure gradients could take place. This would also cause a diurnal variation in wind. However, in the present model we consider only the effect of the diurnal variation in K on the winds and assume that the horizontal pressure gradients are constant in time.

The major problem in the development of a realistic numerical model of diurnal variations of temperature and wind on Mars is the proper choice of the expressions for the eddy exchange coefficients for heat and momentum transport. In the Earth's lower atmosphere, K varies by orders of magnitude in the vertical and over the course of a day. There is no direct theoretical relationship between K and other physical parameters, which would permit a determination of K from first principles. However, for the Earth's atmospheric boundary layer, semi-empirical expressions have been derived relating K to vertical temperature gradient, wind shear, and height above the surface. We shall make use of such expressions in the Martian model. Since K is a function of both wind and temperature, and since wind and temperature depend on K through the vertical eddy transport mechanism, there is a complex interdependence among K, temperature, and wind.

It has been observed in the Earth's atmosphere that there is a thin atmospheric layer adjacent to the surface in which the vertical momentum and heat fluxes vary little (less than 20 percent) with altitude. This layer is called the surface boundary layer or constant flux layer and its thickness is of the order of 50 meters. Above the constant flux layer is a transition layer, of the order of a kilometer in thickness, in which both vertical eddy transport and the horizontal pressure gradients influence the wind. Above the transition layer is the free atmosphere in which the effect of vertical eddy transport decreases and the horizontal pressure gradient is the main factor controlling the wind. We shall make use of this three-zone concept in the Martian model. However, because the radiation fluxes on Mars vary rapidly with height in the lowest atmospheric layer, the assumption of a constant heat flux layer is probably not justified. Therefore, we shall assume that the constant flux layer on Mars applies to momentum but not to heat.

In addition to the three atmospheric zones, there is a subsurface zone in which heat transfer takes place by conduction. The various zones are illustrated in Figure 8. In this diagram z represents height in the atmosphere, z' represents depth in the soil, and the L's represent boundary or interface levels of the various zones.

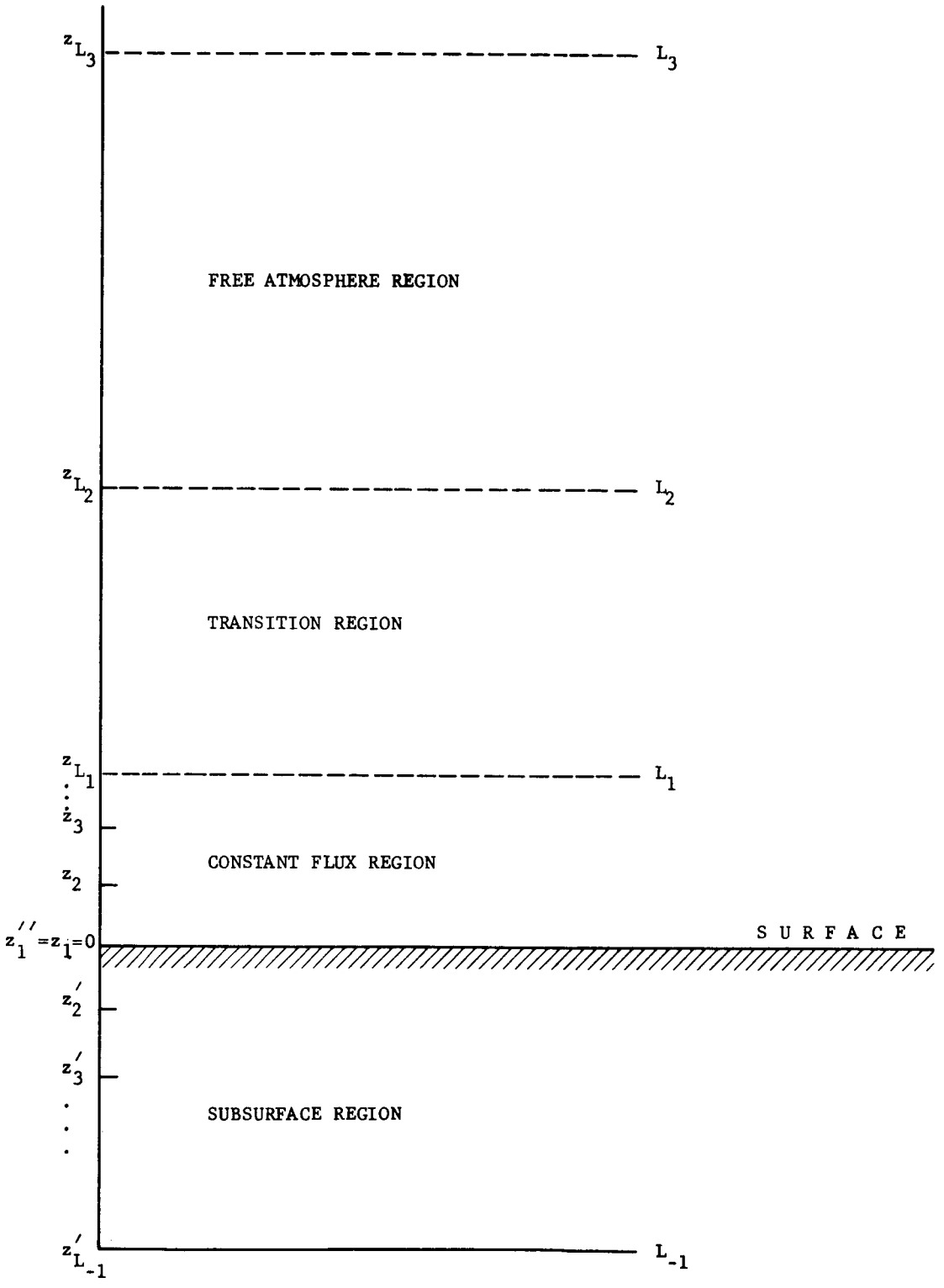

Figure 8. Schematic diagram of the computational model.

4.3.2 Differential Equations for Computing Temperature and Wind Changes. — The differential equations for computing temperature and wind variations in the Martian atmosphere and temperature changes in the soil are as follows.

In the constant flux layer the equations are

$$\left.\begin{aligned} \frac{\partial}{\partial z}\left(K\frac{\partial u}{\partial z}\right) &= 0 \qquad (37)\\ \frac{\partial}{\partial z}\left(K\frac{\partial v}{\partial z}\right) &= 0 \qquad (38)\\ \frac{\partial \theta}{\partial t} &= \frac{\partial}{\partial z}\left(K\frac{\partial \theta}{\partial z}\right) + Q_1 + Q_2 \qquad (39) \end{aligned}\right\} 0 < z \leq L_1$$

where K = eddy exchange coefficient (assumed to be the same for both heat and momentum exchange),
u = west-east velocity component,
v = south-north velocity component,
z = height,
θ = potential temperature,
Q_1, Q_2 = rate of change of temperature due to solar heating and infrared cooling, respectively.

In the transition layer and in the free atmosphere, the equations are

$$\left.\begin{aligned} \frac{\partial u}{\partial t} &= fv - \frac{1}{\rho}\frac{\partial p}{\partial x} + \frac{1}{\rho}\frac{\partial}{\partial z}\left(\rho K\frac{\partial u}{\partial z}\right) \qquad (40)\\ \frac{\partial v}{\partial t} &= -fu - \frac{1}{\rho}\frac{\partial p}{\partial y} + \frac{1}{\rho}\frac{\partial}{\partial z}\left(\rho K\frac{\partial v}{\partial z}\right) \qquad (41)\\ \frac{\partial \theta}{\partial t} &= \frac{1}{\rho}\frac{\partial}{\partial z}\left(\rho K\frac{\partial \theta}{\partial z}\right) + Q_1 + Q_2 \qquad (42) \end{aligned}\right\} L_1 < z \leq L_3$$

where p = pressure,
ρ = density,
f = Coriolis parameter.

It can be seen from the above equations of motion that the advective terms are assumed to be negligible. It is also assumed that the pressure gradients do not change with time.

In the soil the only equation is the heat conduction equation

$$\frac{\partial T'}{\partial t} = \frac{\partial}{\partial z'}\left(K' \frac{\partial T'}{\partial z'}\right) \qquad L_{-1} \leq z < 0 \qquad (43)$$

where T' = soil temperature
K' = thermometric conductivity of soil on Mars.

The expression for eddy heat transfer exchange coefficient K for the constant flux region ($0 < z \leq L_1$) is adopted from Yamamoto and Shimanuki's [24] work for the Earth's atmosphere. For

$$\left.\begin{aligned} &\text{unstable conditions: } K = (kz)^2 \frac{dU}{dz}\left[1 + (\sigma|Ri|)^{\frac{1}{2}}\right] && (44)\\ &\text{stable conditions: } K = (kz)^2 \frac{dU}{dz}\left[1 + (\sigma|Ri|)^{\frac{1}{2}}\left(\frac{L_*}{z}\right)^{p'}\right] && (45)\end{aligned}\right\} \quad 0 < z \leq L_i$$

where k = Von Karman constant = 0.4,
z = height,
$U = (u^2 + v^2)^{\frac{1}{2}}$,
$\sigma = 15$,
$p' = 1/6$,
Ri = Richardson number $= \frac{g}{\theta}\frac{d\theta}{dz}\Big/\left(\frac{du}{dz}\right)^2$,
L_* = modified stability length.

The quantity L_*, a function of the eddy flux of heat, can be determined by an iteration process through the following relation, if Ri and z are known.

$$\frac{(z/L_*)}{\sigma|Ri|} = \frac{1}{\sqrt{1 - (\sigma|Ri|)^{\frac{1}{2}}\,(L_*/z)^{p'}}} \quad . \qquad (46)$$

Now we can determine K for any given height in the constant flux layer. For the transition layer ($L_1 < z \leq L_2$), K is assumed constant with height and equal to the value of K obtained at the top of the constant flux region L_1. For the free atmosphere ($L_2 < z \leq L_3$), K is assumed to decrease linearly with height to a value of zero at L_3.

4.3.3 Boundary Conditions. – The required parameters at the boundaries are evaluated as follows. At the lower boundary of the subsurface region, L_{-1}, it is assumed that the temperature is constant. At the surface, the wind components are equal to zero and the surface temperature θ_g is determined by the following balance equation

$$H_g + F_g\downarrow + S_g\downarrow + G_g = \sigma\, \theta_g^4 \tag{47}$$

where H_g is the heat flux from the atmosphere to the surface by eddy diffusion, $F_g\downarrow$ is the downward infrared flux at the surface, $S_g\downarrow$ is the solar radiation reaching the ground, G_g is the heat flux from the subsurface to the surface by molecular conduction, and σ is Stefan's constant. The heat fluxes comprising the surface balance equation are determined from the following expressions

$$H_g = \rho c_p\, K \left(\frac{\partial T}{\partial z} + \Gamma_{ad} \right)_g \tag{48}$$

$$F_g\downarrow = \int_{\Delta\nu} \int_{\tau_{\nu(top)}}^{1} B_\nu \, d\tau_\nu \, d\nu \tag{49}$$

where the integration over wavenumber ν is preformed over the 15μ CO_2 band and the H_2O rotational band, and $\tau_{\nu(top)}$ represents the transmission from the top of the atmosphere to the surface.

$$S_g\downarrow = \frac{I_o}{R^2} \cos\psi\, (1 - A)(1 - E_g) \tag{50}$$

$$G_g = \rho'\, c'\, K' \left(\frac{\partial T'}{\partial z} \right)_g \tag{51}$$

where ρ' is the soil density and c' the soil specific heat.

At the boundary between the constant flux layer and the transition layer, L_1, the wind components and derivatives of the wind are assumed continuous across the boundary. At the top of the free atmosphere region, L_3, the boundary condition is specified by the temperature rates,

$$\frac{\partial \theta}{\partial t} = Q_1 + Q_2 \tag{52}$$

where Q_1 and Q_2 are the rates of change of temperature due to solar heating and infrared cooling, respectively. For the top of the free atmosphere, these rates are not computed directly but are extrapolated linearly with respect to pressure from the levels below. The wind at the top of the atmosphere is assumed to be constant with time and equal to the geostrophic wind ($u = u_g$; $v = v_g$) at that level.

4.3.4 Numerical Methods. – With the use of an iterative procedure, the equations are solved numerically using unevenly spaced levels in the vertical direction in the atmosphere and evenly spaced levels in the soil. The Martian day is divided into a finite number of intervals of equal length,

$$\Delta t = \frac{t'}{n} \tag{53}$$

where t' is the length of the Martian day, and n is the number of intervals. With a given temperature and wind profile at time $t = 0$, a temperature profile and wind profile for time $t = \Delta t$, is computed. This process is repeated continually until the difference in temperature for a given local time in two successive days is less than some prescribed value, ϵ

$$\theta(t) - \theta(t + t') < \epsilon \ . \tag{54}$$

In describing the numerical procedures we shall make use of the following notation

$$\mu_j^{(n)} \ [k]$$

where μ refers to a parameter such as temperature or wind, j refers to the j-th level in the vertical direction (j increases upwards in the atmosphere and downwards in the soil), n refers to the n-th time step, and k refers to the k-th interation within the n-th time step. For the finite difference analogs of the time rate of change of μ due to diffusive effects (eddy transport in the atmosphere, conduction with the soil) we use the implicit difference equation

$$\frac{3}{2} \ \frac{\mu_j^{(n+1)} - \mu_j^{(n)}}{\Delta t} - \frac{1}{2} \ \frac{\mu_j^{(n)} - \mu_j^{(n-1)}}{\Delta t} = \frac{\delta(K\delta u)_j^{(n+1)}}{\Delta z^2} \ . \tag{55}$$

Since for a given time step (n+1), information for two previous times (n,n-1) are required, two initial profiles are needed to start the computations. Thus, for the first time step, we simply use the explicit difference equation

$$\frac{\mu_j^{(2)} - \mu_j^{(1)}}{\Delta t} = \frac{\delta(K\delta u)_j^{(1)}}{\Delta z^2} \tag{56}$$

where the superscript 1 refers to the beginning of the first time step (initial time) and the superscript 2 to the end of the first time step or beginning of the second time step. Hence, for the subsurface levels (see Equation 43), where K is a constant and the levels are equally spaced, the temperature at the end of the first time step is

$$T_j^{(2)} = T_j^{(1)} + K' \frac{\Delta t}{\Delta z^2} \left(T_{j+1}^{(1)} - 2T_j^{(1)} + T_{j-1}^{(1)} \right) . \tag{57}$$

For the transition layer and free atmosphere, where the levels are not equally spaced, we obtain from the finite difference analog of Equation (40)

$$u_j^{(2)} = u_j^{(1)} + \Delta t \left[fv_j^{(1)} - \left(\frac{1}{\rho} \frac{\partial p}{\partial x} \right)_j + \frac{\rho_{j+\frac{1}{2}}^{(1)} K_{j+\frac{1}{2}}^{(1)} \left(u_{j+1}^{(1)} - u_j^{(1)} \right)}{\rho_j^{(1)} \left(z_{j+1} - z_j \right) \left(z_{j+\frac{1}{2}} - z_{j-\frac{1}{2}} \right)} \right.$$

$$\left. - \frac{\rho_{j-\frac{1}{2}}^{(1)} K_{j-\frac{1}{2}}^{(1)} \left(u_j^{(1)} - u_{j-1}^{(1)} \right)}{\rho_j^{(1)} \left(z_j - z_{j-1} \right) \left(z_{j+\frac{1}{2}} - z_{j-\frac{1}{2}} \right)} \right] \tag{58}$$

where $j+\frac{1}{2}$ refers to the level midway between levels j and j+1. A similar equation may be derived from the v component from Equation (41).

For the entire atmosphere, we obtain from the finite difference analog of the temperature equation (42)

$$\theta_j^{(2)} = \theta_j^{(1)} + \Delta t \left[\frac{\rho_{j+\frac{1}{2}}^{(1)}}{\rho_j^{(1)}} \frac{K_{j+\frac{1}{2}}^{(1)} \left(\theta_{j+1}^{(1)} - \theta_j^{(1)} \right)}{\left(z_{j+1} - z_j \right) \left(z_{j+\frac{1}{2}} - z_{j-\frac{1}{2}} \right)} \right.$$

$$\left. - \frac{\rho_{j-\frac{1}{2}}^{(1)}}{\rho_j^{(1)}} \frac{K_{j-\frac{1}{2}}^{(1)} \left(\theta_j^{(1)} - \theta_{j-1}^{(1)} \right)}{\left(z_{j+1} - z_j \right) \left(z_{j+\frac{1}{2}} - z_{j-\frac{1}{2}} \right)} \right] + \left(Q_1^{(1)} + Q_2^{(1)} \right) \Delta t . \tag{59}$$

The winds in the constant flux region are computed from the finite difference analogs of Equations (37) and (38). Thus,

$$u_{j-1}^{(2)} = \frac{F_x \left(z_j - z_{j-1} \right)}{K_{j-\frac{1}{2}}^{(1)}} \tag{60}$$

where F_x is the constant flux in the x direction, and

$$v_{j-1}^{(2)} = \frac{F_y \left(z_j - z_{j-1} \right)}{K_{j-\frac{1}{2}}^{(1)}} \tag{61}$$

where F_y is the constant flux in the y direction. The values of these fluxes are computed from the first layer of the transition region. Thus,

$$F_x = \frac{K_{L_1+\frac{1}{2}}^{(1)} \left(u_{L_1+1}^{(2)} - u_{L_1}^{(2)} \right)}{\left(z_{L_1+1} - z_{L_1} \right)} \tag{62}$$

$$F_y = \frac{K_{L_1+\frac{1}{2}}^{(1)} \left(v_{L_1+1}^{(2)} - v_{L_1}^{(2)} \right)}{\left(z_{L_1+1} - z_{L_1} \right)} \quad . \tag{63}$$

The surface temperature at n=2 is obtained from the surface balance equation (47), as follows

$$T_g^{(2)} = \left[\frac{F_{g\downarrow}^{(2)} + S_{g\downarrow}^{(2)} + H_g^{(2)} + G_g^{(2)}}{\sigma} \right]^{1/4} . \tag{64}$$

Since $F_g^{(2)}$, $H_g^{(2)}$, and $G_g^{(2)}$ all depend on the surface temperature, a first guess of the magnitudes of these terms is calculated from extrapolations of the atmospheric temperatures and soil temperatures to the surface. Thus, for the atmospheric eddy flux at the surface,

$$H_g^{(2)} = \frac{1}{2} (\rho_1 + \rho_2) c_p \frac{K_2^{(1)}}{2} \left[\frac{T_2^{(2)} - T_g}{z_2} + \Gamma_{ad} \right] \tag{65}$$

where subscript 1 refers to the surface level, subscript 2 to the first level above the surface, T_g is the surface temperature that is obtained from downward linear extrapolation of the atmospheric temperatures computed at levels 2 and 3, $K_2^{(1)}/2$ is the average eddy exchange coefficient of the first atmospheric layer (since $K_1 = 0$). Similarly, for the soil heat flux,

$$G_g^{(2)} = (\rho c)' K' \left(\frac{T_2'^{(2)} - T_g'}{z_2'} \right) \tag{66}$$

where T_g is the surface temperature obtained from upward linear extrapolation of the subsurface temperature.

With these estimates of $H_g^{(2)}$, $G_g^{(2)}$, and a similar one for $F_g{\downarrow}^{(2)}$, a first approximation, $T_g^{(2)}[1]$ is obtained for the surface temperature from Equation (64). $T_g^{(2)}[1]$ is now used to recalculate the surface heat fluxes that depend on it and a second approximation $T_g^{(2)}[2]$ is obtained. The process is iterated until $T_g^{(2)}[k+1] - T_g^{(2)}[k]$ is less than a prescribed value.

At this stage we have two complete initial profiles $[\theta^{(1)}, u^{(1)}, v^{(1)}]$ and $[\theta^{(2)}, u^{(2)}, v^{(2)}]$. For all following time steps ($n + 1 = 3, 4, 5\ldots$), the diffusion type equations are approximated by the implicit difference scheme Equation (55).

The difference equation for heat conduction in the soil is then

$$\frac{3}{2}\frac{T_j^{(n+1)} - T_j^{(n)}}{\Delta t} - \frac{1}{2}\frac{T_j^{(n)} - T_j^{(n-1)}}{\Delta t} = \frac{K'\left(T_{j+1}^{(n+1)} - 2T_j^{(n+1)} + T_{j-1}^{(n+1)}\right)}{\left(z_{j+\frac{1}{2}} - z_{j-\frac{1}{2}}\right)^2} \tag{67}$$

where the primes have been omitted from soil temperatures to simplify the presentation. This equation can be transformed to

$$-A_j T_{j+1}^{(n+1)} + B_j T_j^{(n+1)} - A_j T_{j-1}^{(n+1)} = D_j \tag{68}$$

where

$$A_j = \frac{K'\,\Delta t}{\left(z_{j+\frac{1}{2}} - z_{j-\frac{1}{2}}\right)^2} \tag{69}$$

$$B_j = \frac{3}{2} + \frac{2K'\Delta t}{\left(z_{j+\frac{1}{2}} - z_{j-\frac{1}{2}}\right)^2} \tag{70}$$

$$D_j = 2T_j^{(n)} - \frac{1}{2} T_j^{(n-1)} \quad . \tag{71}$$

Richtmeyer [25] shows how an equation of the form of (68) can be transformed to

$$T_j = E_j T_{j+1} + F_j \tag{72}$$

where superscripts (n+1) on the T's have been omitted for clarity of presentation, and

$$E_j = \frac{A_j}{B_j - A_j E_{j-1}} \tag{73}$$

$$F_j = \frac{D_j + A_j F_{j-1}}{B_j - A_j E_{j-1}} \tag{74}$$

E_j and F_j can be calculated inductively in order of increasing j, starting with the boundary condition at the surface level (j=1) where we have

$$T_1 = E_1 T_2 + F_1 = T_1[1] \tag{75}$$

and, hence,

$$E_1 = 0 \quad \text{and} \quad F_1 = T_1[1] \quad . \tag{76}$$

$T_1[1]$ is a first estimate of surface temperature based upon

$$T_1^{(n+1)}[1] = \left[\frac{F_g^{(n)} + G_g^{(n)} + H_g^{(n)} + S_g^{(n+1)}}{\sigma} \right]^{1/4} . \tag{77}$$

With E_j and F_j calculated, T_j is calculated from Equation (72) starting at the lower boundary of the soil layer where T is a fixed constant and progressing upward in order of decreasing j.

For the eddy transport of heat in the atmosphere, a similar scheme is used. To the temperature change due to eddy heat transport is added the radiational temperature change. Thus, for the atmosphere,

$$\theta_j^{(n+1)} = \left(\theta_j^{(n+1)}\right)_{\text{Eddy}} + (Q_j^n)\Delta t$$

where $\left(\theta_j^{(n+1)}\right)_{\text{Eddy}}$ is the temperature that would be produced by eddy heat exchange and $(Q_j^n)\Delta t$ is the additional temperature change due to radiational processes. In the calculation of $\left(\theta_j^{(n+1)}\right)_{\text{Eddy}}$, $K_j^{(n)}$ is used.

For the wind at time step (n+1), n = 2, 3, ..., in the transition region and free atmosphere, the implicit difference equation corresponding to Equation (40) is

$$\frac{\frac{3}{2}\left(u_j^{(n+1)} - u_j^{(n)}\right)}{\Delta t} - \frac{\frac{1}{2}\left(u_j^{(n)} - u_j^{(n-1)}\right)}{\Delta t} = fv_j^{(n)} - \left(\frac{1}{\rho}\frac{\partial p}{\partial x}\right)_j$$

$$+ \frac{\rho_{j+\frac{1}{2}}^{(n)}}{\rho_j^{(n)}} \frac{K_{j+\frac{1}{2}}^{(n)}\left(u_{j+1}^{(n+1)} - u_j^{(n+1)}\right)}{\left(z_{j+1} - z_j\right)\left(z_{j+\frac{1}{2}} - z_{j-\frac{1}{2}}\right)} - \frac{\rho_{j-\frac{1}{2}}^{(n)}}{\rho_j^{(n)}} \frac{K_{j-\frac{1}{2}}^{(n)}\left(u_j^{(n+1)} - u_{j-1}^{(n+1)}\right)}{\left(z_j - z_{j-1}\right)\left(z_{j+\frac{1}{2}} - z_{j-\frac{1}{2}}\right)} \quad (78)$$

Letting

$$A_j = \frac{\rho_{j+\frac{1}{2}}^{(n)}}{\rho_j^{(n)}} \frac{K_{j+\frac{1}{2}}^{(n)} \Delta t}{\left(z_{j+1} - z_j\right)\left(z_{j+\frac{1}{2}} - z_{j-\frac{1}{2}}\right)}$$

$$B_j = \frac{3}{2} + \left[\frac{\rho_{j+\frac{1}{2}}^{(n)}}{\rho_j^{(n)}} \frac{K_{j+\frac{1}{2}}^{(n)}}{\left(z_{j+1} - z_j\right)\left(z_{j+\frac{1}{2}} - z_{j-\frac{1}{2}}\right)} + \frac{\rho_{j-\frac{1}{2}}^{(n)}}{\rho_j^{(n)}} \frac{K_{j-\frac{1}{2}}^{(n)}}{\left(z_j - z_{j-1}\right)\left(z_{j+\frac{1}{2}} - z_{j-\frac{1}{2}}\right)}\right] \Delta t \quad (79)$$

$$C_j = \left[\frac{\rho_{j-\frac{1}{2}}^{(n)}}{\rho_j^{(n)}} \frac{K_{j-\frac{1}{2}}^{(n)}}{\left(z_j - z_{j-1}\right)\left(z_{j+\frac{1}{2}} - z_{j-\frac{1}{2}}\right)}\right] \Delta t \quad (80)$$

$$D_j = 2u_j^{(n)} - \frac{1}{2} u_j^{(n-1)} + \left[fv_j^{(n)} - \left(\frac{1}{\rho}\frac{\partial p}{\partial x}\right)_j\right] \Delta t \quad (81)$$

we can transform Equation (78) to

$$-A_j u_{j+1}^{(n+1)} + B_j u_j^{(n+1)} - C_j u_j^{(n-1)} = D_j \quad . \quad (82)$$

Equation (82) is solved with the use of Richtmeyer's [25] technique, subject to the boundary conditions at the top of the free atmosphere, $u = u_g$, and the boundary condition at the base of the transition layer,

$$\frac{\left(u_{L_1+1}^{(n+1)} - u_{L_1}^{(n+1)}\right)}{\left(z_{L_1+1} - z_{L_1}\right)} K_{L_1+\frac{1}{2}}^{(n)} = F_x^{(n)} \quad . \tag{83}$$

A similar procedure applies to the v component of the wind.

The winds in the constant flux layer and the surface temperature for all time steps are computed with the same procedures described previously for the first time step.

All radiational terms are computed using the methods described in Sections 2 and 4.2.

4.3.5 Input Parameters. – There are a number of input parameters for the model. These include latitude, solar declination, solar isolation at the top of the Martian atmosphere, and planetary albedo; specific heat, molecular weight, CO_2 and H_2O mixing ratios, surface pressure, and adiabatic lapse rate of the atmosphere; specific heat, density, thermal diffusivity of the Martian soil; the thicknesses of the constant flux region and transition region, and the number and spacing of the levels in each of the atmospheric regions; the number of levels and the temperature at the lowest level of the Martian subsurface region; the initial wind and temperature profiles; and the time step and convergence criteria.

Most of these parameters are known or can be estimated. However, there are two parameters that are really unknown for Mars, and those may significantly affect the results of any computation of diurnal variations. These are the thickness of the constant flux layer and the thickness of the transition layer. A series of computations in which these two parameters are varied can be performed to determine the sensitivity of Martian diurnal variations to their choice.

4.3.6 Test of Computational Model. – Preliminary experiments with different time steps indicated that a time step of five minutes would yield no instabilities. These experiments were conducted with nine atmospheric levels (including the surface).

A run was then attempted to calculate the diurnal variation of temperature and wind at 40° north latitude at the time of the northern hemisphere winter solstice. The other input parameters for this run were: planetary albedo, 0.30 ; solar insolation at top of the atmosphere,

7.22×10^5 erg cm^{-2} sec^{-1}; $c_p = 8.58 \times 10^6$ erg g^{-1} deg^{-1}; CO_2 percentage by mass, 61 percent; H_2O mixing ratio, 0; surface pressure, 10 mb; molecular weight of the atmosphere, 35.8; adiabatic lapse rate, 4.35°K/km; specific heat of soil, 1.26×10^7 erg g^{-1}; soil density, 1 g cm^{-3}; thermal diffusivity of soil, 7×10^{-5} cm^2 sec^{-1}; temperature of lowest level of soil, 210°K; time step, 5 minutes; and surface temperature iteration convergence criterion, 1°. The initial atmospheric and soil profiles are shown in Table 8. Also shown in Table 8 are the fixed pressure gradients computed from the geostrophic wind equation applied to the initial winds, and the separation of the various regions of the atmosphere. The initial wind profile is derived from interpolation and extrapolation of the winds computed by Leovy and Mintz [26] for this latitude and time of year in their numerical general circulation experiment for Mars. Thus, their wind profile and the horizontal pressure gradient associated with it should be representative of the large-scale flow. The calculations should reveal the diurnal variations about the large-scale flow that is introduced by a diurnally varying eddy mixing process.

The calculations were started at 9 a.m. local Martian time and run for twenty-four hours, or short of a full Martian day of twenty-four hours, thirty-seven minutes. The calculations ran smoothly until about 4 p.m. in the afternoon. At this time an unstable oscillation developed in the eddy mixing coefficient and in the winds. Preliminary analysis of the cause of this oscillation suggests that it is due to the change in formula used to compute the eddy mixing coefficient when the Richardson number changes from negative to positive, or from unstable to stable conditions [see Equations (44) and (45)]. The change in formula leads to a discontinuity in the eddy mixing coefficient from one time step to the next. This discontinuity apparently leads to the unstable oscillation. Further analysis of this instability will be performed.

The temperature variation at several atmospheric levels up to the time that the instability arose is plotted in Figure 9. Also shown in Figure 9 is the computed surface temperature for the entire twenty-four hour run; the surface temperatures after 16 hours are uncertain because of the oscillation in K at that time and are, therefore, shown as a dashed line. The lag in the time of maximum temperature with height is evident in the curves. The computed eddy mixing coefficients during the time period 9 to 16 hours were of the order of 10^5 cm^2 sec^{-1}.

Also obtained for the first seven hours of the run are the u and v components of the wind and the subsurface temperatures. At the present time, these results are still undergoing analysis. However, preliminary analysis suggests that the treatment of the constant momentum flux boundary condition at the interface between the constant flux region and the transition region can be improved. There is also apparently an error in the v component computations, whose source is, at present, undetermined.

The problem areas discussed above will be thoroughly analyzed before proceeding with further computations with the variable K model.

TABLE 8

INITIAL ATMOSPHERIC AND SOIL PROFILES, AND FIXED PRESSURE GRADIENTS FOR CALCULATION OF DIURNAL VARIATIONS ON MARS AT LATITUDE 40°N, NORTHERN HEMISPHERE WINTER SOLSTICE

	ATMOSPHERE							SOIL	
Region	p (mb)	z (m)	T (°K)	u (m sec^{-1})	v (m sec^{-1})	dp/dy (dynes cm^{-3})	dp/dx (dynes cm^{-3})	Depth (cm)	T (°K)
	10.0	0	192	0	0			0	192
Constant Flux	9.99	12	184	1.7	-0.5			2	187
———————	9.98	24	182	1.9	-0.6	-4.2×10^{-7}	-1.3×10^{-7}	4	191
	9.97	35	181	2.1	-0.6	-4.7×10^{-7}	-1.3×10^{-7}	6	196
Transition	9.71	340	181	11.1	-2.1	-2.6×10^{-6}	-4.8×10^{-7}	8	210
———————	9.50	580	180	24.9	-1.1	-5.7×10^{-6}	-2.5×10^{-7}		
	7.57	3,000	169	31.0	-0.8	-6.0×10^{-6}	-1.5×10^{-7}		
Free Atmosphere	5.03	7,000	155	47.0	-0.2	-6.6×10^{-6}	-2.0×10^{-8}		
	1.10	20,000	134	100.0	6.0	-3.5×10^{-6}	$+2.1 \times 10^{-7}$		

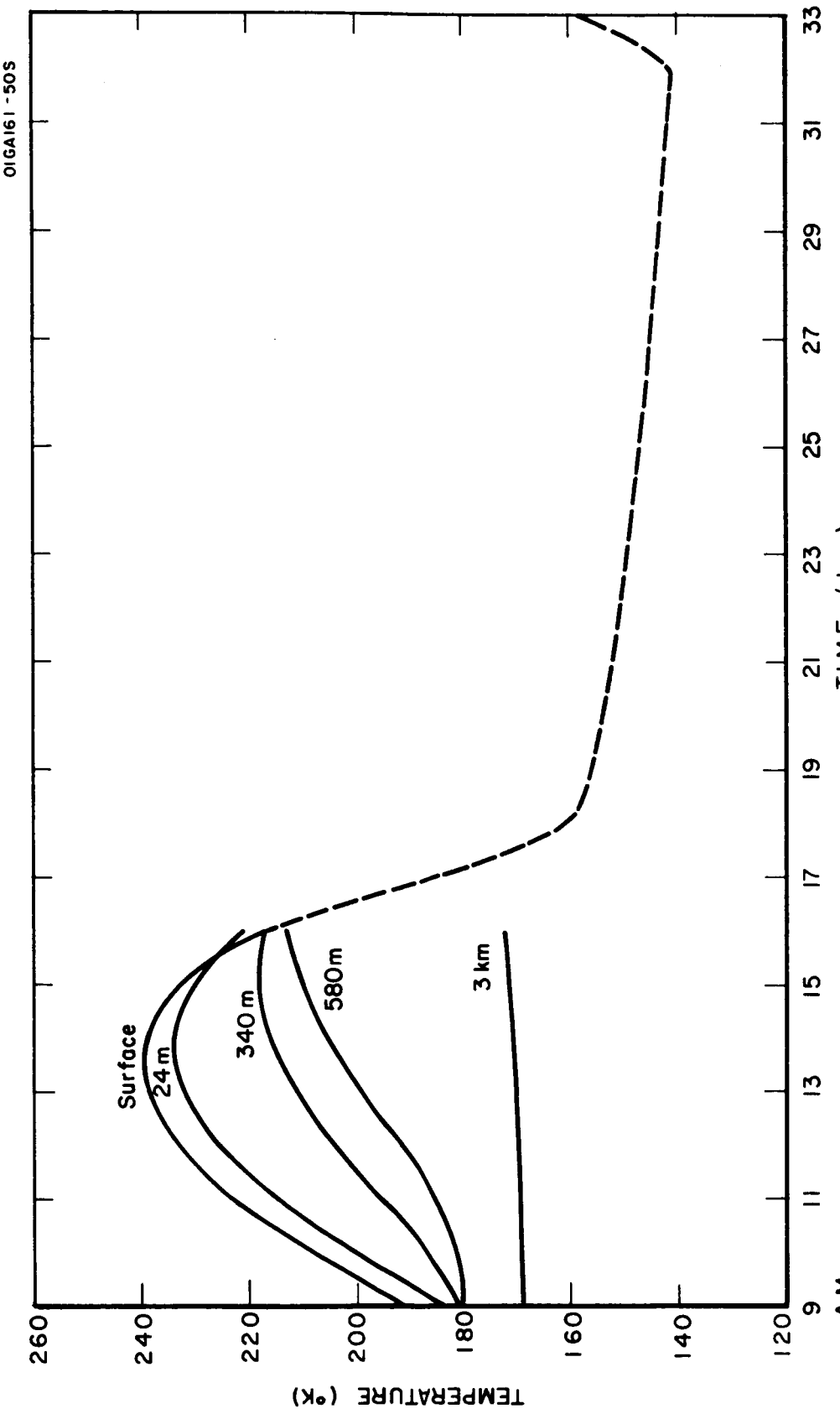

Figure 9. Temperature variations at several atmospheric levels for first seven hours and at surface for twenty-four hours of experimental run. (Latitude, 40°N; solar declination, + 24°).

4.4 Concluding Remarks

A constant K model for computing the diurnal variation of temperatures on Mars has been developed. The model includes both radiative heat transfer and eddy heat transfer in the atmosphere and conduction within the soil. Calculations were performed of the diurnal temperature variation at the Martian equator at the time of the northern hemisphere spring equinox. An atmospheric eddy mixing coefficient, K, of 10^4 cm^2 sec^{-1} was assumed. The results indicate that the diurnal temperature range at ~1.5 km is about 12 percent of the surface diurnal range while at ~3 km it is about 3 percent of the surface diurnal range.

The development of a variable K model for computing diurnal variations of atmospheric temperatures and winds, and diurnal variations of surface and subsurface temperatures on Mars has been described. In this model the eddy mixing coefficient is computed from a semi-empirical formula relating K to height above the ground, wind shear, and Richardson number. The model also assumes an atmospheric constant flux layer adjacent to the surface in which the flux of momentum is constant with altitude. The results of test computations with this model indicate several problem areas, which are still undergoing analysis at this writing.

REFERENCES

1. Ohring, G., W. Tang, and J. Mariano, "Planetary Meteorology", NASA-CR-85569, 68 pp. (1967).

2. Ohring, G., "Radiative Transfer and the Thermal Structure of Planetary Atmosphere," GCA-TR-67-18-N, Contract No. NASW-1574, 32 pp. (1967).

3. Manabe, S., and R.F. Strickler, "Thermal Equilibrium of the Atmosphere with Convective Adjustment," J. Atmos. Sci., 21, 361-385 (1964).

4. Rodgers, C.D., and C.D. Walshaw, "The Computation of Infrared Cooling Rates in Planetary Atmospheres," Quart. J. Roy. Meteorol. Soc., 92, 67-92 (1966).

5. Pivovonsky, M., and M.R. Nagel, Tables of Blackbody Radiation Functions, MacMillan, New York, 481 pp. (1961).

6. Houghton, J.T., "The Absorption of Solar Infrared Radiation by the Lower Stratosphere,"Quart. J. Roy. Meteorol. Soc., 89, 319-331 (1963).

7. Kaplan, L., G. Münch, and H. Spinrad, "An Analysis of the Spectrum of Mars,"Astrophys. J., 139, 1-15 (1964).

8. Schorn, R., H. Spinrad, R. Moore, H. Smith, and L. Giver, "High Dispersion Spectroscopic Observations of Mars. II. The Water Vapor Variations," Astrophys. J., 147, 743-752.

9. Dollfus, A., "Mesure de la quantité de vapeur d'eau contenue dans l'atmosphère de la planète Mars," Compt. Rend., 256, 3009-3011 (1963).

10. Dollfus, A., "Analyse des mesures de la quantité de vapeur d'eau dans l'atmosphère de la planète Mars," Compt. Rend., 261, 1603-1606 (1965).

11. Kliore, A., D. Cain, G. Levy, V. Eshleman, G. Fjeldbo, and F. Drake, "Occultation Experiment: Results of the First Direct Measurements of Mars Atmosphere and Ionosphere," Science, 149, 1243-1248 (1965).

12. Belton, M.J., and D.M. Hunten, "The Abundance and Temperature of CO_2 in the Martian Atmosphere," Astrophys. J., 145, 454-467 (1966).

13. Owen, T., "The Composition and Surface Pressure of the Martian Atmosphere: Results from the 1965 Opposition," Astrophys. J., 146, 257-270 (1966).

14. Spinrad, H., R.A. Schorn, R. Moore, L.P. Giver, and H.J. Smith, "High-Dispersion Spectroscopic Observations of Mars. I. The CO_2 Content and Surface Pressure," Astrophys. J., 146, 331-338 (1966).

15. House, F., G. Ohring, C. Sherman, and W. Tang, "Study of the Martian Atmospheric Environmental Requirements for Spacecraft and Entry Vehicles," Final Report, JPL Contract No. 951767, GCA Tech. Report No. 67-12-G, 159 pp. (1967).

16. London, J., "A Study of the Atmospheric Heat Balance," OTS No. PB 129551, 99 pp. (1957).

17. Sinton, W.M., and J. Strong, "Radiometric Observations of Mars," Astrophys. J., 131, 459-469 (1960).

18. Goody, R., and M.J. Belton, "Radiative Relaxation Times for Mars: A Discussion of Martian Atmospheric Dynamics," Planet. Space Sci., 15, 247-256 (1967).

19. Neubauer, F., "Thermal Convection in the Martian Atmosphere,"J. Geophys. Res., 71, 2419-2428 (1966).

20. Leovy, C., "Radiative-Convective Equilibrium Calculations for a Two-Layer Mars Atmosphere," Rand Memo. RM-5017, 41 pp. (1966).

21. Fisher, E., "A Theoretical Study of the Sea Breeze," J. Meteor. 18, 216-233 (1961).

22. Leovy, C., "Note on Thermal Properties of Mars," Rand Memo. RM-4551-NASA, 17 pp. (1965).

23. Haurwitz, B., Dynamic Meteorology. McGraw-Hill Book Co., Inc., New York, 365 pp. (1941).

24. Yamamoto, G., and A. Shimanuki, "Turbulent Transfer in Diabatic Conditions," J. Meteorol. Soc., Japan, 44, 301-307 (1966).

25. Richtmyer, R.D., Difference Methods for Initial Value Problems. Interscience, New York, 238 pp. (1957).

26. Leovy, C., and Y. Mintz, "A Numerical General Circulation Experiment for the Atmosphere of Mars," Rand Memo. No. RM-5110-NASA, under Contract NASr-21, (1966).